RESEARCH MEMORANDUM

PERFORMANCE CHARACTERISTICS OF AIRCRAFT COOLING EJECTORS HAVING SHORT CYLINDRICAL SHROUDS

By Fred D. Kochendorfer and Morris D. Rousso

Lewis Flight Propulsion Laboratory
Cleveland, Ohio

NATIONAL ADVISORY COMMITTEE
FOR AERONAUTICS

WASHINGTON

May 22, 1951

NATIONAL ADVISORY COMMITTEE FOR AERONAUTICS

RESEARCH MEMORANDUM

PERFORMANCE CHARACTERISTICS OF AIRCRAFT COOLING EJECTORS HAVING SHORT CYLINDRICAL SHROUDS

By Fred D. Kochendorfer and Morris D. Rousso

SUMMARY

The factors affecting the performance of ejectors suitable for aircraft cooling are investigated theoretically and experimentally. The investigation covers a range of shroud-to-nozzle diameter ratios from 1.1 to 1.6, of shroud lengths from 0.2 to 2.28 nozzle diameters, of secondary-to-primary weight-flow ratios from 0 to 0.12, and of ambient-to-nozzle pressure ratios from 0.7 to 0.06.

It is shown that for low values of the ratio of the jet ambient pressure to the nozzle-inlet total pressure the primary jet expands to a supersonic velocity as it leaves the nozzle. For the case with no secondary flow, the expansion continues until the jet strikes the shroud wall and a stable supersonic flow in which the primary stream completely fills the shroud is established. With secondary flow, both streams accelerate until the secondary Mach number equals unity, that is, until the shroud "chokes." In both cases the flow up to the shroud section for which the expansion ceases is relatively independent of mixing effects.

The results of a simplified theoretical analysis based on each type of flow are in good agreement with those experimentally obtained.

INTRODUCTION

Ejectors are currently being considered to provide combustion-chamber and tail-pipe cooling for high-speed jet aircraft because they may meet the cooling requirements with little loss or possibly with some gain in thrust characteristics. The usual advantages of ejectors over other pumping devices - lightness and simplicity of construction and maintenance - are also important factors.

Various design considerations distinguish the ejector suitable for aircraft cooling from the type commonly employed heretofore. A cooling ejector must pump a small amount of cooling air (probably about 5 percent of the combustion air) through a small pressure rise. In fact, depending on the type of cooling-air intake employed and on the ducting

losses, a pressure drop may be available for an appreciable range of flight speeds. One of the most important geometrical requirements for an aircraft installation is that the shroud or mixing section be as short as possible. In addition, current aircraft design practice usually includes a convergent primary nozzle rather than the convergent-divergent type commonly used with industrial ejectors. As a result of these differences, few existing performance data are applicable to the design of aircraft ejectors.

An investigation of cooling ejectors is therefore being conducted at the NACA Lewis laboratory. The performance of short, conical-shroud ejectors reported in references 1 and 2 represents the first phase of these studies. The internal flow is studied herein in detail to gain an understanding of the operating principles. In order to simplify the internal flow as much as possible, cylindrical shrouds were employed.

The investigation covered a range of shroud-to-nozzle diameter ratios from 1.10 to 1.60, shroud lengths up to 2.28 nozzle diameters, secondary-to-primary weight-flow ratios from 0 to 12 percent, and ambient-to-primary pressure ratios from 0.7 to 0.06.

SYMBOLS

The following symbols are used in this report:

A	area
a	area ratio, A_s/A_p
C	constant
D	diameter
g	acceleration of gravity
L	shroud length
$(L/D_p)_c$	critical shroud length
M	Mach number
P	total pressure
p	static pressure
$(P_s/P_p)_m$	minimum ejector pressure ratio

$(p_0/P_p)_b$	break-off primary pressure ratio
R	gas constant
T	total temperature
V	velocity
w	weight flow
x	distance downstream of nozzle exit, primary diameters
α	area ratio, A_1/A_p
γ	ratio of specific heats
ρ	mass density
τ	temperature ratio, T_s/T_p
ω	weight-flow ratio, w_s/w_p

Subscripts:

p	primary stream at nozzle exit
s	secondary stream at nozzle exit
w	shroud wall
0	jet ambient conditions
1	primary stream after acceleration
2	secondary stream after acceleration

APPARATUS AND PROCEDURE

The ejector apparatus schematically shown in figure 1 consisted of four interchangeable primary nozzles, a plate containing the outer wall of the secondary passage, a secondary chamber, and a number of cylindrical interlocking shroud rings.

[redacted]

[redacted]

All shroud rings had an inside diameter of 1.40 inches. By selecting the proper rings, the total shroud length could be varied from 0 to 4.0 inches in 0.25-inch increments. Shroud-wall pressure orifices were 0.020-inch diameter holes spaced 0.25 inch between centers.

The throat diameters of the primary nozzles were such that the available secondary-to-primary diameter ratios were 1.10, 1.20, 1.40, and 1.60. The constant-area throat sections were 1.5 inches long. A preliminary test showed that the total-pressure loss through the nozzle was less than 0.4 percent of the inlet total pressure for all nozzles. Consequently, the primary total pressure was assumed to be atmospheric.

The secondary passage was designed so that the secondary stream entered the shroud almost axially. At the shroud entrance, the angles between the center line and a tangent to the outside and inside surfaces of the passage were 0° and 5°, respectively. A check on the secondary flow near the shroud entrance showed that the curvature of the passage resulted in a static-pressure difference between the inside and outside passage walls of about 0.4 percent of the average static pressure. The passage friction loss was found to be less than 0.5 percent of the secondary-chamber total pressure for all required secondary flows. The chamber pressure was therefore used as a measure of the secondary total pressure.

The ejector assembly was mounted on a low-pressure receiver having an 8- by 9-inch cross section. The receiver was connected to the laboratory exhauster system; any pressure between 2 inches of mercury absolute and atmospheric could be obtained by throttling. The jet ambient pressure was measured by four static orifices in the receiver wall.

Atmospheric air was used as both the primary and secondary fluid. The primary air entered the nozzle directly from the room, whereas the secondary air passed through a calibrated rotameter and a throttling valve and was then divided into two streams that entered the secondary chamber at diametrically opposite points.

During the course of the preliminary investigation, humidity was found to affect ejector performance; this effect, although small, was not negligible if reproducible results were to be obtained. It was found that if the air used had a temperature of $70 \pm 5^\circ$ F and a dew point of $20 \pm 10^\circ$ F the spread in data in no case exceeded 2 percent. Consequently, these limitations were used for all runs reported herein.

For each ejector configuration, the secondary weight flow was held constant and the jet ambient pressure was varied in steps from a low value to a value such that the primary nozzle was just choked, that is, to a value such that the ratio of the shroud-wall static pressure for the orifice nearest the primary nozzle exit to the primary total pressure equalled 0.528. This limitation frequently resulted in ambient-to-primary total-pressure ratios as large as 0.7. For each value of the ambient pressure, readings of the shroud wall pressures and of the secondary total pressure were taken.

EXPERIMENTAL RESULTS

The experimental ejector-performance curves are presented in figures 2 to 5 for shroud-to-nozzle diameter ratios of 1.60, 1.40, 1.20, and 1.10, respectively. For each curve the ejector pressure ratio P_s/P_p is shown as a function of the primary pressure ratio p_0/P_p for a constant value of the weight-flow parameter $\omega\sqrt{\tau}$, which is defined as the ratio of secondary-to-primary weight flows multiplied by the square root of the ratio of secondary-to-primary total temperatures. Although the primary and secondary temperatures were equal ($\tau = 1$) for all runs reported herein, $\omega\sqrt{\tau}$ will subsequently be shown to be the proper variable for short ejectors.

An inspection of figures 2 to 5 shows that for the lower values of the primary pressure ratio the ejector pressure ratio for each curve is independent of the primary pressure ratio and represents the minimum value obtainable for the particular value of the weight-flow parameter. As the primary pressure ratio is increased a value, which will be hereinafter called the break-off pressure ratio, is reached for which the ejector pressure ratio increases. It can be seen that at break-off the abruptness of the change in ejector pressure ratio decreases with increasing values of the weight-flow parameter. For values above break-off, the ejector pressure ratio increases almost linearly with the primary pressure ratio.

Because of the irregularity of the performance curves, the selection of an ejector to fulfill specific cooling requirements will involve a careful evaluation of the effects of ejector geometry on performance. For example, at a constant ejector pressure ratio an increase in the diameter ratio or a decrease in the shroud length results in an increase in the weight-flow parameter for primary pressure ratios less than break-off, but usually results in a decrease in the weight-flow parameter for pressure ratios greater than break-off.

In order to illustrate these effects, the flight performance of a few typical ejectors was determined. In all cases it was assumed that

the efficiency of primary diffusion was 0.95 and that the total pressure ratio across the engine was 2.0. Secondary-diffuser efficiencies were taken as 0 and 0.6. Curves of weight-flow parameter as a function of primary pressure ratio or flight Mach number are presented in figure 6. The effects of changes in diameter ratio can be found by comparing curves A and B or C and D. For the assumed conditions, increasing the diameter ratio increases the weight-flow parameter over the entire range of flight Mach numbers. On the other hand, the effects of increasing the shroud length (curves A and C or B and D) are such that the weight-flow parameter is increased for low Mach numbers and decreased for high Mach numbers. If the efficiency of secondary diffusion is increased to 0.6 (curves E and F), the curves intersect at a lower Mach number and the shorter ejector has a greater pumping ability over a large part of the Mach number range. Obviously, there is no "best" ejector. Even when cooling requirements are specified, the choice may not be clear cut, particularly when the effect of ejector geometry on the net thrust minus drag is considered.

ANALYSIS AND DISCUSSION

Examination of the experimental curves shows that ejector performance for the lower values of primary pressure ratio will be completely determined if the factors that affect the values of the minimum ejector pressure ratio and the break-off pressure ratio can be evaluated. Some characteristics of the internal shroud flow can be immediately seen. The fact that the ejector pressure ratio can be independent of the primary pressure ratio indicates that a sonic or supersonic flow is established in which the primary and secondary streams completely fill the shroud. The abrupt change in ejector pressure ratio that occurs for low values of the weight-flow parameter is further evidence of supersonic flow because this is exactly the characteristic that would result from the passage of a shock upstream to the section at which the expanding primary stream meets the shroud. In addition, the fact that decreasing the shroud length resulted in an increase in the weight-flow parameter suggests that mixing is not the principal factor affecting ejector performance for low primary pressure ratios.

An idealized flow will be assumed in which the primary stream expands to some lower pressure as it leaves the nozzle and establishes a condition of supersonic flow. Mixing effects will be neglected. The cases with and without secondary flow will be discussed separately. In each case, the first step in the analysis will be to compare the characteristics of an idealized frictionless flow with those experimentally observed. If the agreement is good, the next step will be to compare the experimental results quantitatively with those obtained by applying the equations of conservation of mass and momentum to the idealized flow.

No Secondary Flow

If the expanding primary jet strikes the shroud wall and establishes a stable supersonic flow in which the stream completely fills the shroud, the general effects of variations in the primary pressure ratio upon the shroud-wall-pressure distribution should be similar to those observed with convergent-divergent nozzles.

Experimental shroud-wall-pressure distributions for several values of the primary pressure ratio are shown in figure 7 for a typical ejector. The curves illustrate the effect of primary pressure ratio upon the wall-pressure distribution.

For low values of the primary pressure ratio, the internal flow is completely supersonic, the ejector pressure ratio is equal to $(P_s/P_p)_m$, and the wall-pressure distribution (curve A) is independent of the primary pressure ratio. The peak in the wall-pressure curve ($x \approx 0.4$) marks the position of the oblique shock that results when the primary stream strikes the wall. As the primary pressure ratio increases, the wall pressures in the downstream section of the shroud are affected by shocks that move upstream. Because the flow in the upstream section is still supersonic, however, the ejector pressure ratio remains equal to $(P_s/P_p)_m$. When the primary pressure ratio reaches break-off, the shock has moved upstream to the section at which the stream strikes the wall and the wall-pressure distribution (curve B) therefore represents the maximum pressure ratio that can exist at each station for a flow in which the stream fills the shroud. As the value of the primary pressure ratio increases above break-off, the stream can no longer fill the shroud, an annulus of semidead air surrounds the jet, and the ejector pressure ratio increases abruptly (curve C).

If the primary pressure ratio is decreased from a value greater than break-off, the order of events may not be completely reversed. Above break-off the pressure ratio that governs the amount of primary expansion (that is, the ejector pressure ratio) is less than the primary pressure ratio by a factor that depends on the amount of mixing. A decrease in the primary pressure ratio causes a greater decrease in the ejector pressure ratio because the increased expansion results in larger shear forces. A primary pressure ratio is finally reached for which the flow is unstable to small disturbances and changes abruptly to the type in which the stream fills the shroud. Because the criterions that determine this pressure ratio are quite different from those that determine the break-off pressure ratio, the two ratios may not be equal and hysteresis may result. As would be expected, the effect is most pronounced for cases having the least shear, that is, for large diameter ratios and small shroud-length ratios. Examples of hysteresis can be seen in figures 2(a) and 2(b).

[redacted]

Because the wall-pressure distributions confirm the assumed flow, it is reasonable to compare quantitatively the results of an analysis based on the assumed flow with those experimentally observed. The one-dimensional equations for conservation of mass and momentum can be written for the section of the shroud between the primary-nozzle exit and a hypothetical station at which the stream fills the tube and the Mach number M_1 and pressure p_1 are uniform (section between stations I and II, fig. 8). If a value is assumed for P_1/P_p, both M_1 and $(P_s/P_p)_m$ then become functions of the diameter ratio D_s/D_p.

The difference between p_1 and P_s depends on the wall friction, which in turn depends on the flow that circulates in the region between the shroud wall and the expanding jet. Because the jet strikes the wall within a relatively short distance ($x \approx 0.4$ for the case of fig. 7), however, mixing effects and the resulting wall friction should be small and it can be assumed that

$$P_1/P_p \cong (P_s/P_p)_m$$

Although the value of the minimum ejector pressure ratio is independent of shroud length for the preceding analysis, an internal flow of the type assumed cannot exist unless the shroud is long enough to intercept the expanding jet. The minimum ejector pressure ratio should therefore be independent of shroud length only for shroud lengths longer than a critical value $(L/D_p)_c$ that depends upon the diameter ratio. For shroud lengths shorter than the critical value, it is reasonable to assume that the minimum ejector pressure ratio is the value corresponding to a Prandtl-Meyer expansion through an angle such that the jet just strikes the shroud exit.

The details of the calculation based upon the assumptions are presented in appendix A and a comparison of theory and experiment (experimental values from figs. 2 to 5) is given in figure 9. The theoretical values for shroud lengths both longer and shorter than the critical length are seen to be in good agreement with the corresponding experimental values.

If the maximum value of the primary pressure ratio for which the assumed flow can exist can now be determined, the ejector characteristics for low primary pressure ratios will be completely explained. The difference between the value of the break-off pressure ratio and the value of the minimum ejector pressure ratio is due to the considerable pressure rise resulting from the shock configuration within the shroud. Because the value of the shroud Mach number M_1 is known from the preceding analysis, the pressure increase resulting from a normal shock at this Mach number can be found as a function of the diameter ratio. The

details of the calculation are presented in appendix A and a comparison of the theoretical and experimental values of the break-off pressure ratio is given in figure 10. Also included are experimental wall-pressure distributions at break-off conditions (similar to curve B of fig. 7) for relatively long shrouds ($L/D_p \approx 4$). As would be expected, the wall-pressure curves for the long shrouds can be used to estimate break-off pressure ratios for shorter shrouds. For shroud-length ratios or downstream distances greater than 1.0, the experimental curves approach values that are in good agreement with normal-shock theory. The fact that lengths of at least 1 shroud diameter are required to obtain the pressure increase corresponding to a normal shock is in agreement with the observations of other experimenters. (See, for example, reference 3.)

Although for primary pressure ratios less than break-off, ejector characteristics can be explained by a flow in which friction and mixing effects are neglected, the difference between the primary pressure ratio and the ejector pressure ratio for curve C of figure 7 is evidence that mixing between the primary core and the semidead air region has an important effect on the performance characteristics for primary pressure ratios greater than break-off. As a result, ejector performance is relatively dependent on shroud length for the higher primary pressure ratios. At a diameter ratio of 1.20, for example, increasing the shroud-length ratio from 0.43 to 1.29 (figs. 4(b) and 4(e)) causes a decrease of more than 20 percent in the ejector pressure ratio for a primary pressure ratio greater than break-off, whereas the same increase in shroud length changes the ejector pressure ratio by only 5 percent for low primary pressure ratios. For primary pressure ratios such that $(p_0/P_p)_b < p_0/P_p < 0.7$, mixing effects are almost independent of pressure ratio and the ejector pressure ratio is given by

$$P_s/P_p \cong p_0/P_p - C \qquad (1)$$

where C depends only on ejector configurations.

Secondary Flow

Because the static pressure of the secondary stream is ordinarily lower than that of the primary for the station at the primary-nozzle exit, the primary stream expands as it leaves the nozzle. Because this expansion reduces the secondary-flow area, the secondary stream accelerates and, if it is assumed that little energy exchange occurs, the pressure drops causing a further expansion of the primary.

It has been shown that along a curve of constant weight flow the ejector pressure ratio becomes independent of the primary pressure

[redacted]

ratio. Consequently, the streams must accelerate until the secondary Mach number equals unity and the shroud "chokes." So far, the process does not depend on mixing. It should be noted, however, that secondary acceleration beyond sonic velocity is impossible in a constant-area shroud unless accompanied by energy exchange.

Wall-pressure distributions can again be used as a check on the assumed flow. The curves of figure 11 are typical of the experimental distributions for ejectors with secondary flow. For low primary pressure ratios, the wall-pressure distribution (curve A) is independent of primary pressure ratio and the ejector pressure equals its minimum value. The sharp increase in wall-pressure ratio observed for the case with no secondary flow (fig. 7) is absent and the wall-pressure ratio drops with downstream distance in accordance with the assumed flow. As the primary pressure ratio increases above that corresponding to curve A, a shock moves upstream into the primary core. Because mixing effects are probably small, the secondary Mach number cannot be much greater than unity and the pressure rise required of the secondary stream must be obtained principally by diffusion. During this process the flow area of the secondary stream increases and that of the primary decreases the requirement of constant total area can therefore be satisfied. At break-off (curve B), the pressure rise of the secondary stream equals the maximum value available from the combined effects of mixing and diffusion. Consequently, any further increase in the primary pressure ratio requires an increase in the ejector pressure ratio. For the ejector and weight-flow condition of figure 10, the ejector pressure ratio does not change abruptly but increases almost linearly with primary pressure ratio. In addition, the combined effects of mixing and diffusion are such that the break off pressure ratio approximately equals the minimum ejector pressure ratio; that is, the over-all effect is the same as that which would result if the secondary stream were diffused isentropically to zero velocity.

In order to obtain quantititive results for the assumed flow, the conditions for conservation of mass and momentum are employed for the section of the shroud between stations I and II (fig. 12). As in the case of no secondary flow, if an assumption is made as to the pressure at the downstream station, the value of $(P_s/P_p)_m$ can be obtained as a function of $\omega\sqrt{\tau}$ and D_s/D_p. The fact that the wall-pressure curve of figure 11 is smooth and continuous for the region near the nozzle exit suggests that the primary expansion may be nearly isentropic. An analysis based on the proposed flow and on the assumption that the primary flow is isentropic up to the section at which the secondary Mach number equals unity is presented in appendix B and the results are given in figure 13. The curves represent the theoretical variation of the minimum ejector pressure ratio with diameter ratio for several values of the weight-flow parameter. For completeness the values for $\omega\sqrt{\tau} = 0$ are also included.

The theoretical and experimental values are compared in figure 14. As in the case of no flow, a value of the shroud-length ratio exists beyond which the experimental values of the minimum ejector pressure are independent of shroud-length ratio. The experimental values for shroud lengths greater than critical are in good agreement with the corresponding theoretical values. For the range of the variables covered in the investigation, the assumption of isentropic primary expansion therefore appears to be justified.

Because the maximum pressure increase that can be supported by the secondary fluid depends on the amount of mixing between the primary and secondary streams and on the amount of secondary diffusion that can be accommodated, no simple analytical method for the determination of the value of the break-off pressure ratio could be found for the case of secondary flow.

In a similar manner, the relation between the ejector pressure ratio and the primary pressure ratio for values of primary pressure ratio greater than break-off depends on the effects of mixing and diffusion. In general, equation (1) is still valid but the value of the constant C depends on the weight-flow parameter as well as on the ejector configuration.

SUMMARY OF RESULTS

The following results were obtained in an investigation of aircraft cooling ejectors having short cylindrical shrouds:

1. For low values of the ratio of the jet ambient pressure to the primary total pressure, the performance of aircraft cooling ejectors could be adequately explained by the methods of nonviscous fluid mechanics. Mixing effects could be neglected.

2. When no secondary flow existed, the expanding primary jet struck the shroud wall and established a stable supersonic flow in which the stream completely filled the shroud. The Mach number of the expanded flow and the ejector pressure ratio depended only on the ratio of the shroud to nozzle diameters except for the very short shroud lengths. The ejector pressure ratio was independent of the primary pressure ratio until the primary pressure ratio reached a value corresponding to a normal shock at the expanded Mach number. The supersonic flow then broke down and the stream no longer filled the shroud.

3. For the case of secondary flow, both streams accelerated until a condition was reached such that the secondary Mach number was unity. The ejector pressure ratio depended upon the ratio of secondary-to-primary weight flow, the ratio of secondary to primary temperature, and the diameter ratio.

[redacted]

4. The theoretical values obtained by employing the equations for conservation of mass and momentum were in good agreement with the corresponding experimental values.

Lewis Flight Propulsion Laboratory,
National Advisory Committee for Aeronautics,
Cleveland, Ohio.

[redacted]

APPENDIX A - EJECTOR THEORY - NO SECONDARY FLOW

Shroud-Length Ratios Greater Than $(L/D_p)_c$

The one-dimensional equations for the conservation of mass and momentum is written for the section of the shroud between stations I and II (fig. 8). First, in accordance with the proposed flow, the following assumptions can be made:

(1) Adiabatic flow, $T_p = T_1$

(2) $p_1/P_p = (P_s/P_p)_m$

(3) $M_p = 1$

Let $a = A_s/A_p \equiv (D_s/D_p)^2$. The equation for the conservation of mass is then

$$w_p = w_1$$

or

$$p_p\sqrt{\frac{\gamma+1}{2}} = ap_1M_1\sqrt{1 + \frac{\gamma-1}{2}M_1^2} \tag{2}$$

and the equation for the conservation of momentum is

$$p_p + \rho_pV_p^2 + (a-1)p_1 = ap_1 + a\rho_1V_1^2$$

or

$$p_p(1+\gamma) + (a-1)p_1 = ap_1(1+\gamma M_1^2) \tag{3}$$

Equations (2) and (3) can be combined to give

$$\left.\begin{aligned} a &= \frac{1}{M_1\sqrt{2(\gamma+1)\left(1 + \frac{\gamma-1}{2}M_1^2\right) - \gamma M_1^2}} \\ p_1/P_p &= \frac{\sqrt{\left(\frac{2}{\gamma+1}\right)^{\frac{\gamma+1}{\gamma-1}}}}{aM_1\sqrt{1 + \frac{\gamma-1}{2}M_1^2}} \end{aligned}\right\} \tag{4}$$

[redacted]

The method of solution is as follows:

(1) Assume M_1

(2) Calculate a and $p_1/P_p = (P_s/P_p)_m$ from equation (4)

The corresponding value of the break-off pressure ratio can then be found as follows:

(1) Find static-pressure ratio across normal shock at M_1, p_y/p_x

(2) Calculate $(p_0/P_p)_b = (p_1/P_p)(p_y/p_x)$

The ratios $(p_0/P_p)_b$ and $(P_s/P_p)_m$ are now known as functions of a and therefore as functions of the diameter ratio D_s/D_p.

Shroud Lengths Less Than $(L/D_p)_c$

Assume that the primary fluid undergoes a Prandtl-Meyer expansion such that it just strikes the shroud exit. Assume also that for the diameter ratios under consideration two-dimensional flow is sufficiently accurate.

Then $(P_s/P_p)_m$ is the pressure ratio corresponding to an expansion through an angle ν (see for example, reference 4), where

$$\nu = \tan^{-1} \frac{D_s/D_p - 1}{2\ L/D_p}$$

The ratio $(P_s/P_p)_m$ is thus a known function of D_s/D_p and L/D_p.

APPENDIX B - EJECTOR THEORY - SECONDARY FLOW

The equations for the conservation of mass and momentum will be written for the section of the shroud between stations I and II (fig. 12). The following assumptions will be made:

(1) $p_2 = p_1$

(2) $M_p = M_2 = 1$

(3) No energy interchange, $T_p = T_1$ and $T_s = T_2$

(4) Primary expansion is isentropic

Let $a = A_s/A_p$ and $\alpha = A_1/A_p$; conservation of mass for the primary stream is then

$$\sqrt{\frac{R}{\gamma g}}\frac{w_p\sqrt{T_p}}{A_p} = p_p\sqrt{\frac{\gamma+1}{2}} = \alpha p_1 M_1\sqrt{1+\frac{\gamma-1}{2}M_1^2} \tag{5}$$

and for the secondary stream

$$\sqrt{\frac{R}{\gamma g}}\frac{w_s\sqrt{T_s}}{A_p} = (a-1)p_s M_s\sqrt{1+\frac{\gamma-1}{2}M_s^2} = (a-\alpha)p_1\sqrt{\frac{\gamma+1}{2}} \tag{6}$$

Conservation of momentum for the combined flow is

$$\left(p_p+\rho_p V_p^2\right)+(a-1)\left(p_s+\rho_s V_s^2\right) = \alpha\left(p_1+\rho_1 V_1^2\right)+(a-\alpha)\left(p_1+\rho_2 V_2^2\right)$$

or

$$p_p(1+\gamma)+(a-1)p_s(1+\gamma M_s^2) = \alpha p_1(1+\gamma M_1^2)+(a-\alpha)p_1(1+\gamma) \tag{7}$$

Equations (5), (6), and (7) can be combined to give

$$\omega\sqrt{\tau} = P_s/P_p\,\frac{(a-1)}{(A/A^*)_s} = (a-\alpha)\,p_1/p_p = \frac{(F/F^*)_1-1}{(F/F^*)_s-1} \tag{8}$$

where

[redacted]

$$F/F^* = \frac{1 + \gamma M^2}{M\sqrt{2(\gamma+1)\left(1 + \frac{\gamma-1}{2}\right)M^2}}$$

and

$$A/A^* = \frac{1}{M}\sqrt{\left[\frac{2\left(1 + \frac{\gamma-1}{2}M^2\right)}{\gamma+1}\right]^{\frac{\gamma+1}{\gamma-1}}}$$

The method of solution is as follows:

(1) Assume M_1 and M_s

(2) Compute $\alpha = (A/A^*)_1$, $p_1/P_p = \left(1 + \frac{\gamma-1}{2} M_1^2\right)^{\frac{\gamma}{\gamma-1}}$, $(F/F^*)_1$, $(F/F^*)_s$, and $(A/A^*)_s$

(3) Compute $\omega\sqrt{\tau} = (F/F^*)_1 - 1/(F/F^*)_s - 1$

(4) Compute $a = \left(\frac{2}{\gamma+1}\right)^{\frac{\gamma}{\gamma-1}} \omega\sqrt{\tau}\, \frac{P_p}{P_1} + \alpha$

(5) Compute $(P_s/P_p)_m = \frac{\omega\sqrt{\tau}\,(A/A^*)_s}{a-1}$

Because the values of $(P_s/P_p)_m$, a, and $\omega\sqrt{\tau}$ can be obtained for any assumed set of values for M_1 and M_s, $(P_s/P_p)_m$ can be obtained as a function of a and $\omega\sqrt{\tau}$.

REFERENCES

1. Huddleston, S. C., Wilsted, H. D., and Ellis, C. W.: Performance of Several Air Ejectors with Conical Mixing Sections and Small Secondary Flow Rates. NACA RM E8D23, 1948.

2. Wilsted, H. D., Huddleston, S. C., and Ellis, C. W.: Effect of Temperature on Performance of Several Ejector Configurations. NACA RM E9E16, 1949.

3. Bailey, N. P.: Abrupt Energy Transformation in Flowing Gases. A.S.M.E. Trans., vol. 69, no. 7, Oct. 1947, pp. 749-757; discussion, pp. 758-763.

4. The Staff of the Ames 1- by 3-Foot Supersonic Wind-Tunnel Section: Notes and Tables for Use in the Analysis of Supersonic Flow. NACA TN 1428, 1947.

[redacted]

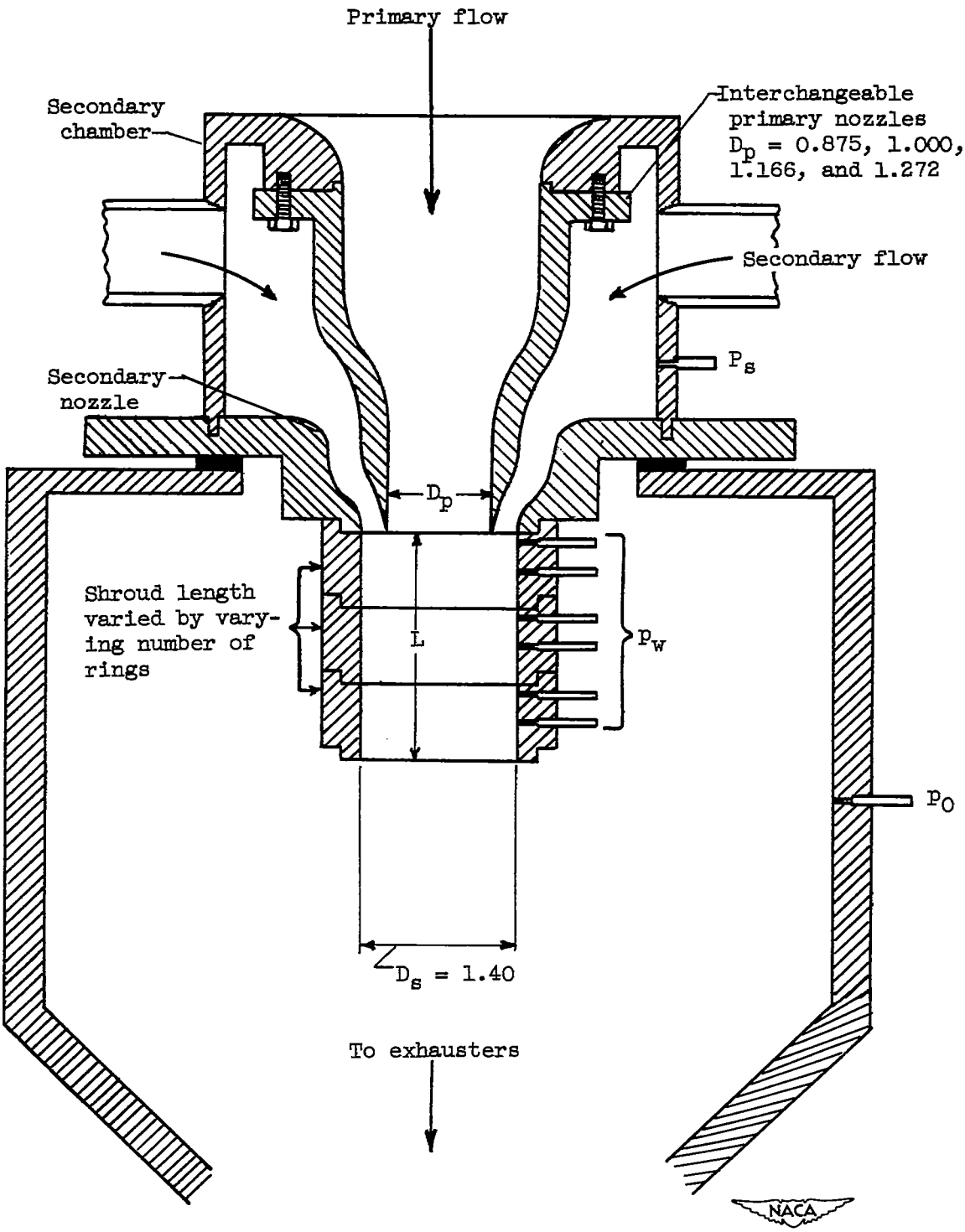

Figure 1. - Diagram of ejector apparatus.

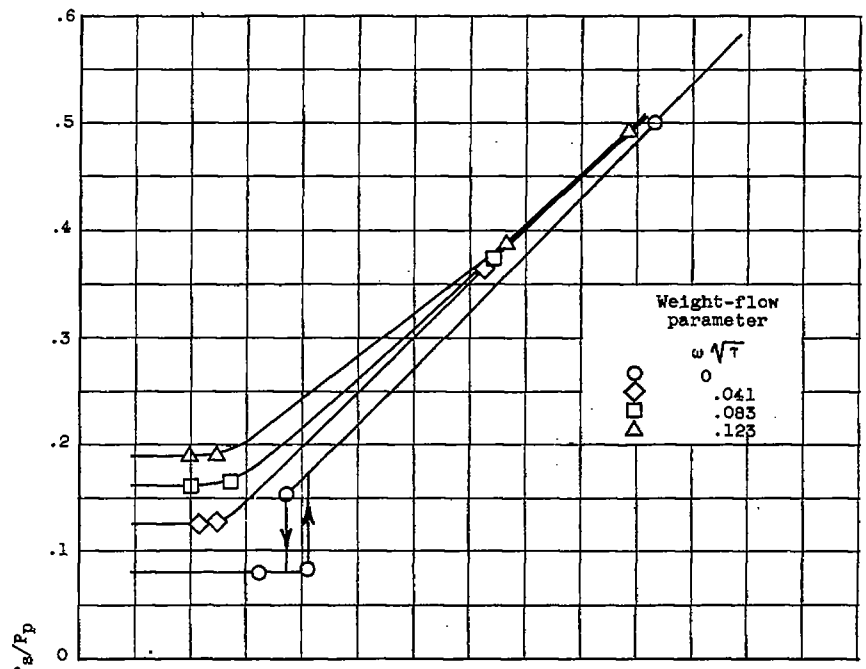

(a) Shroud-length ratio, L/D_p, 0.57.

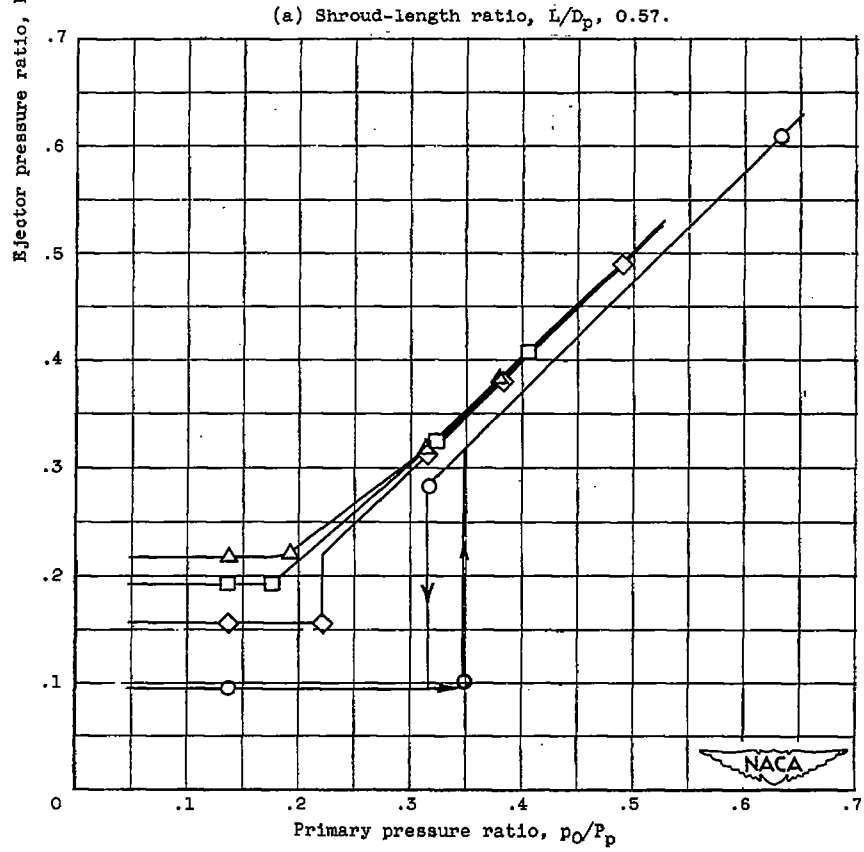

(b) Shroud-length ratio, L/D_p, 1.14.

Figure 2. - Ejector performance curves. Diameter ratio D_s/D_p, 1.60.

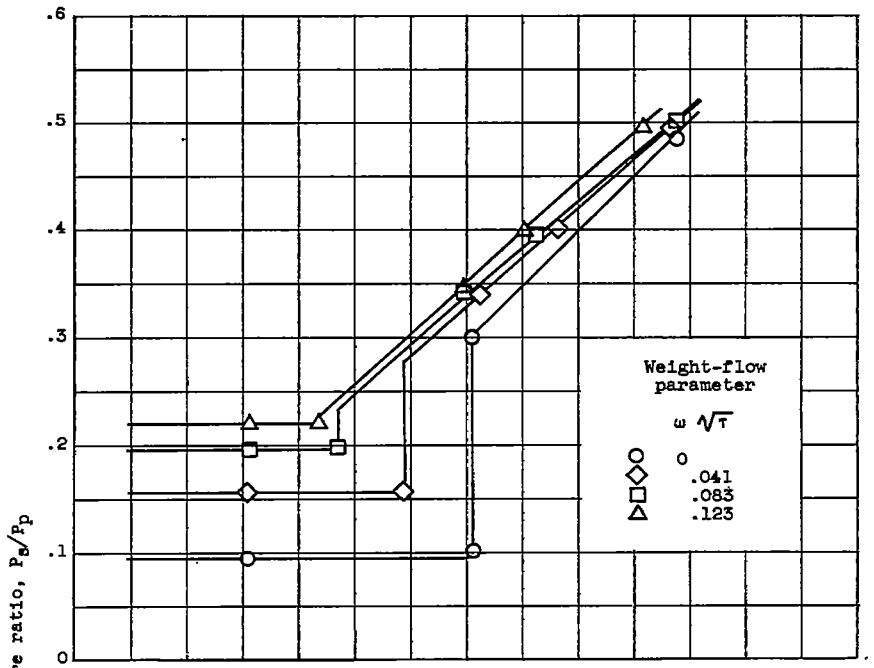

(c) Shroud-length ratio, L/D_p, 1.71.

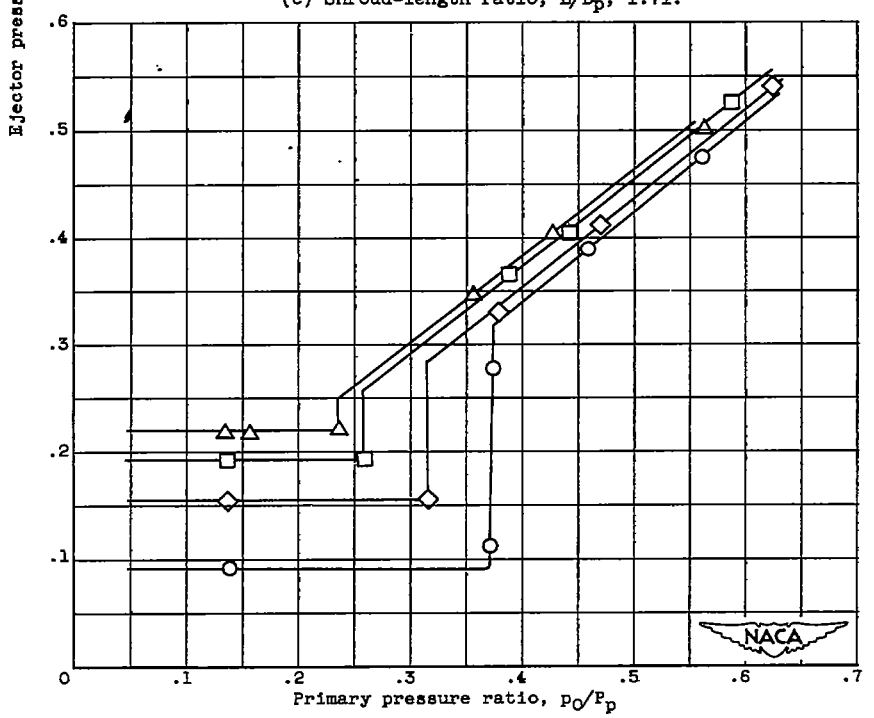

(d) Shroud-length ratio, L/D_p, 2.28.

Figure 2. - Concluded. Ejector performance curves. Diameter ratio D_s/D_p, 1.60.

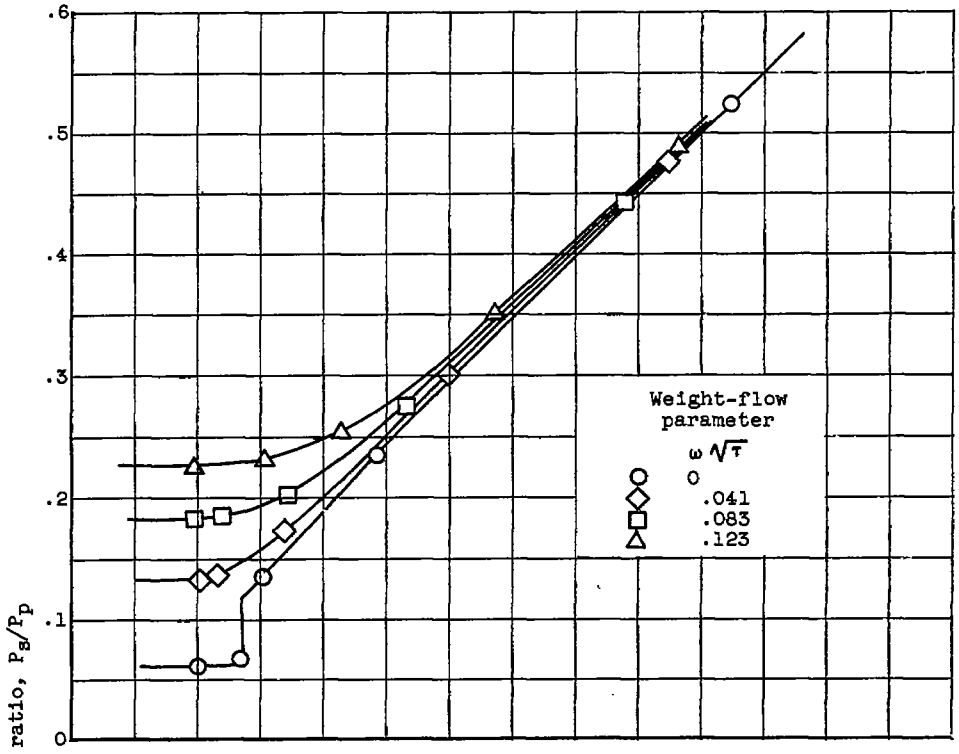

(a) Shroud-length ratio, L/D_p, 0.25.

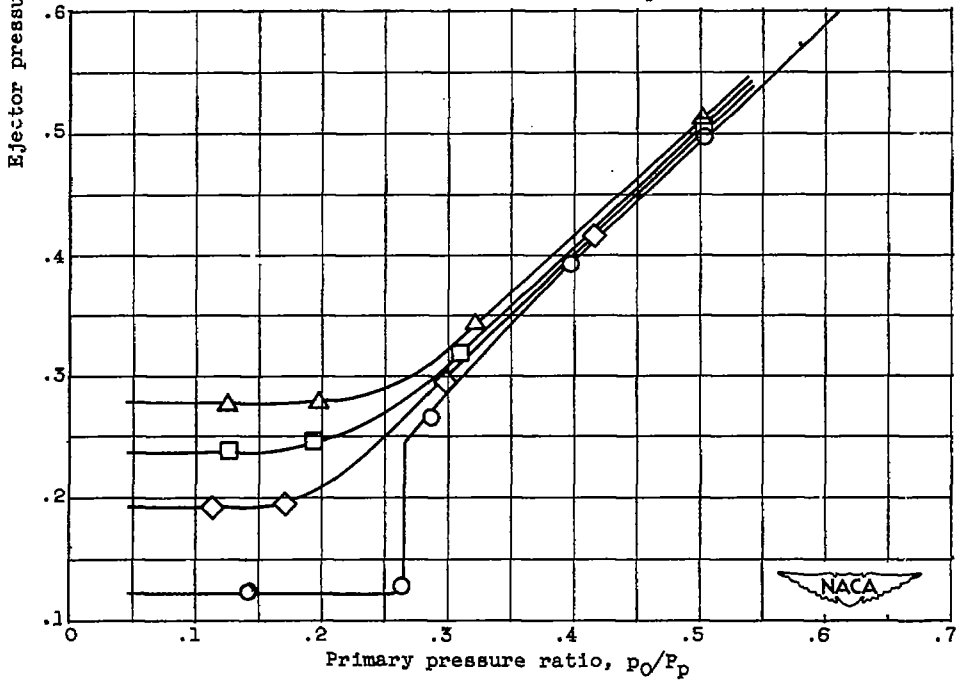

(b) Shroud-length ratio, L/D_p, 0.5.

Figure 3. - Ejector performance curves. Diameter ratio D_s/D_p, 1.40.

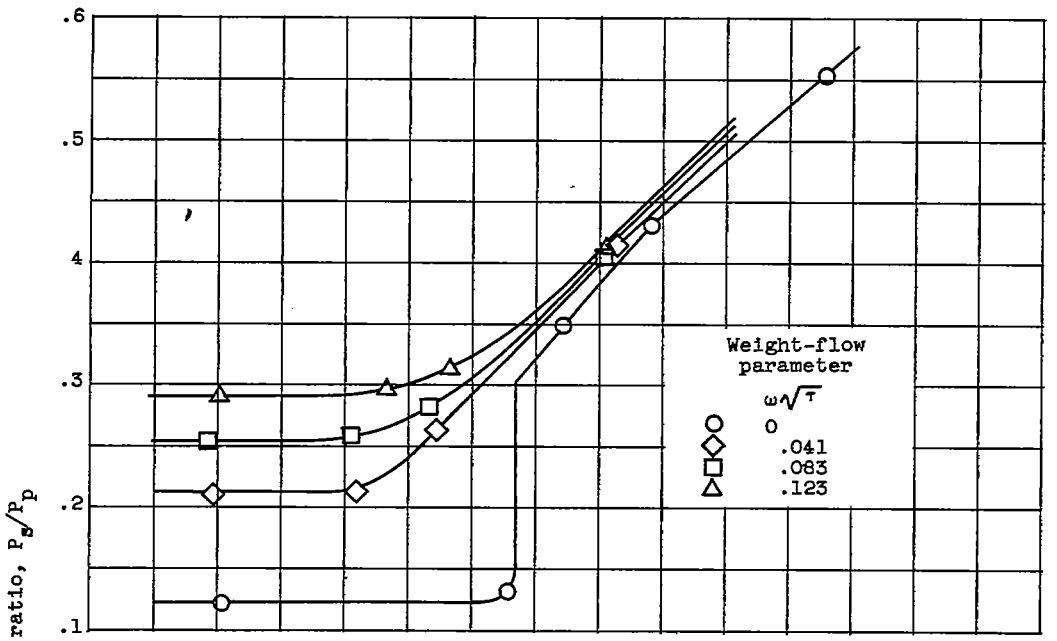

(c) Shroud-length ratio, L/D_p, 0.75.

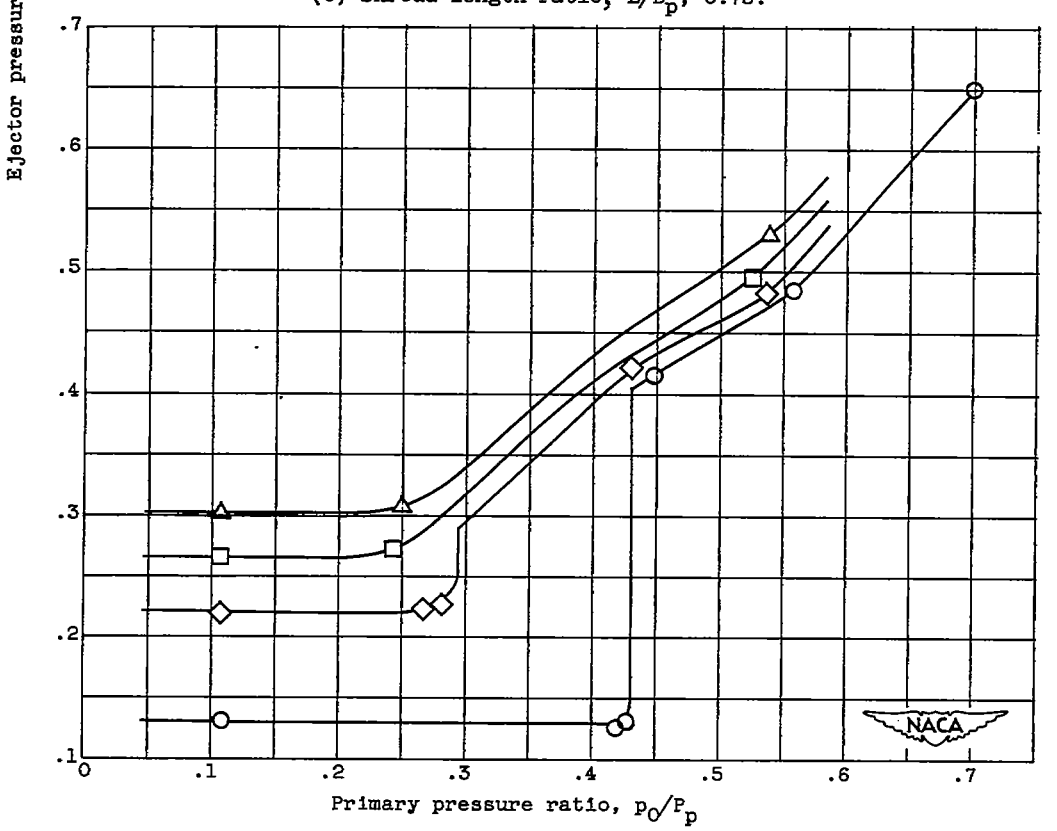

(d) Shroud-length ratio, L/D_p, 1.0.

Figure 3. - Continued. Ejector performance curves. Diameter ratio, D_s/D_p, 1.40.

[redacted]

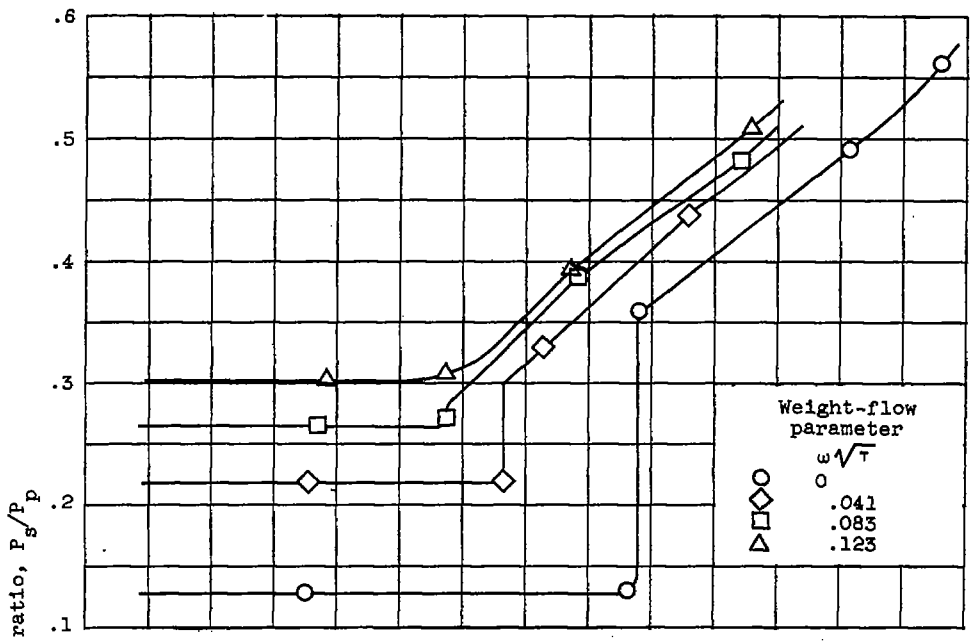

(e) Shroud-length ratio, L/D_p, 1.50.

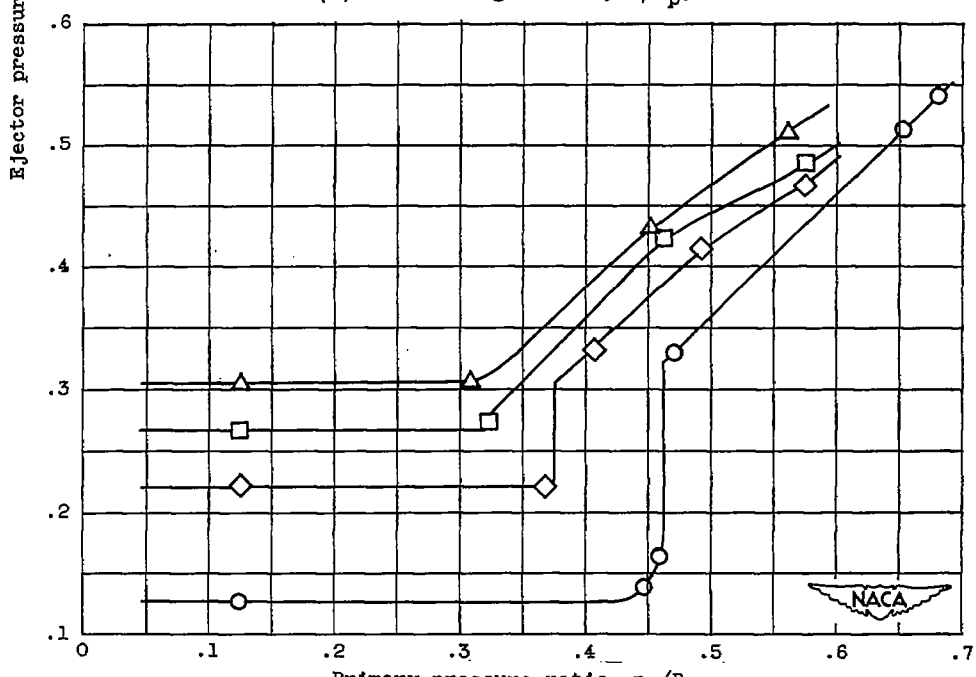

(f) Shroud-length ratio, L/D_p, 2.0.

Figure 3. - Concluded. Ejector performance curves. Diameter ratio, D_s/D_p, 1.40.

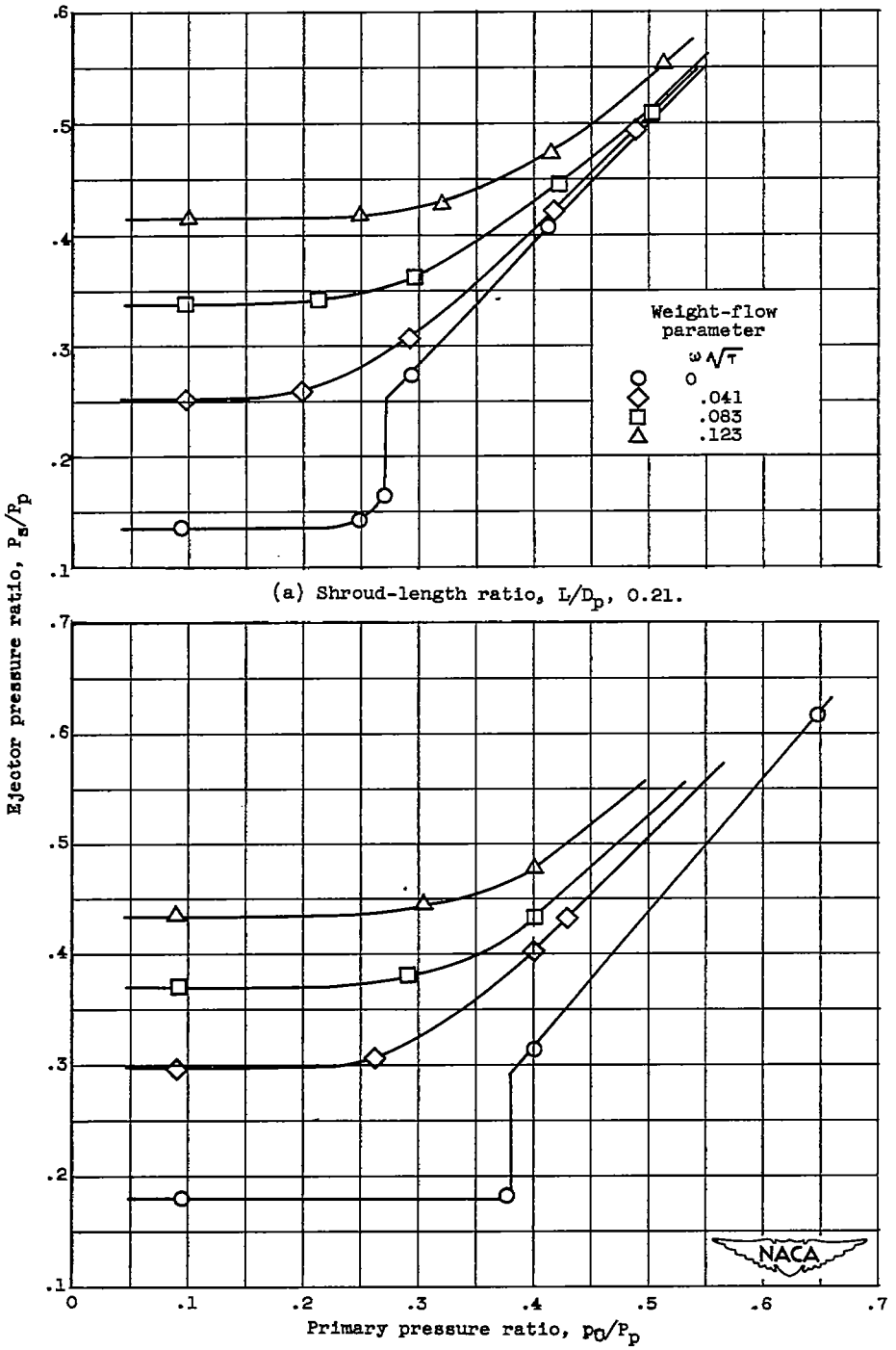

(a) Shroud-length ratio, L/D_p, 0.21.

(b) Shroud-length ratio, L/D_p, 0.43.

Figure 4. - Ejector performance curves. Diameter ratio D_s/D_p, 1.20.

[redacted]

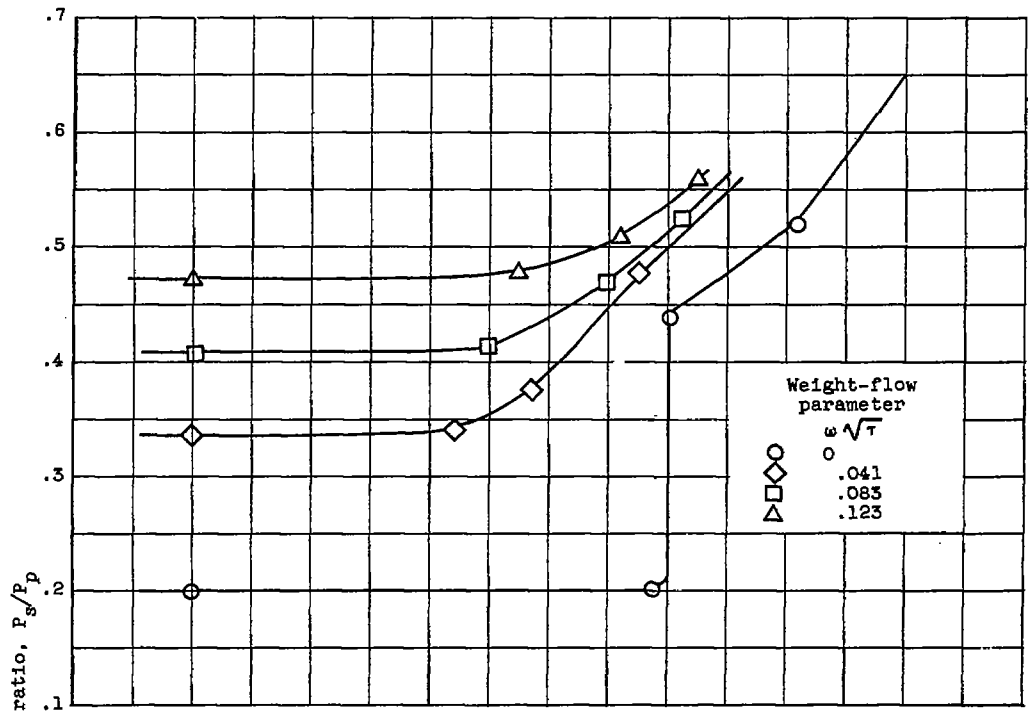

(c) Shroud-length ratio, L/D_p, 0.64.

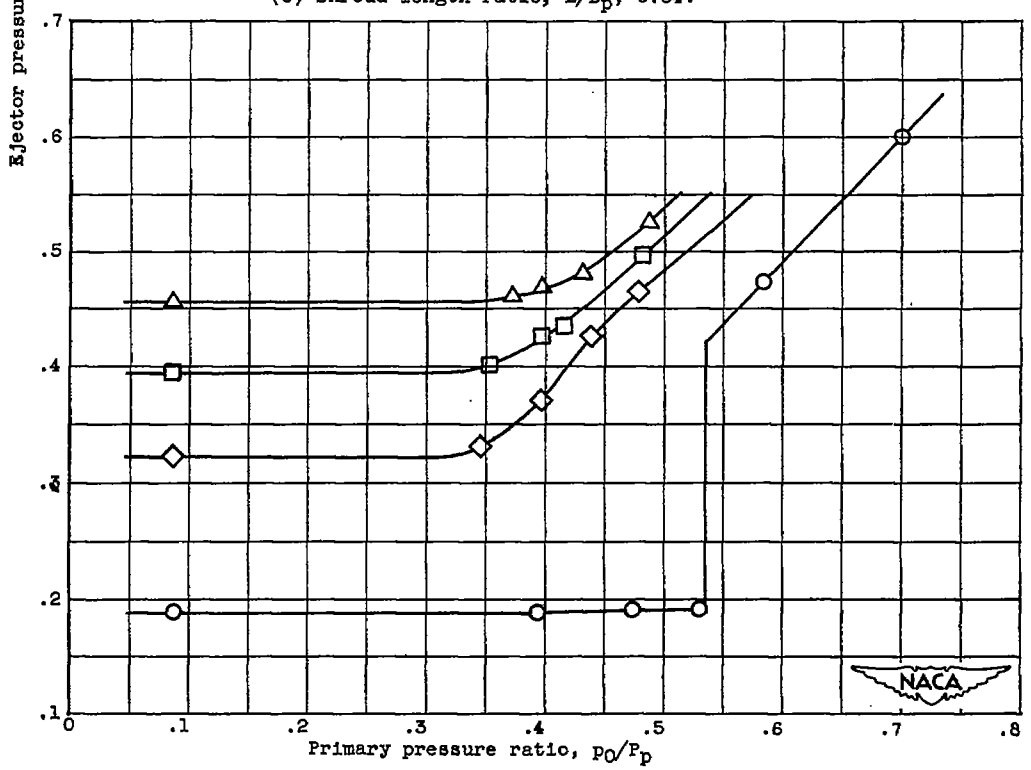

(d) Shroud-length ratio, L/D_p, 0.86.

Figure 4. - Continued. Ejector performance curves. Diameter ratio D_s/D_p, 1.20.

[redacted]

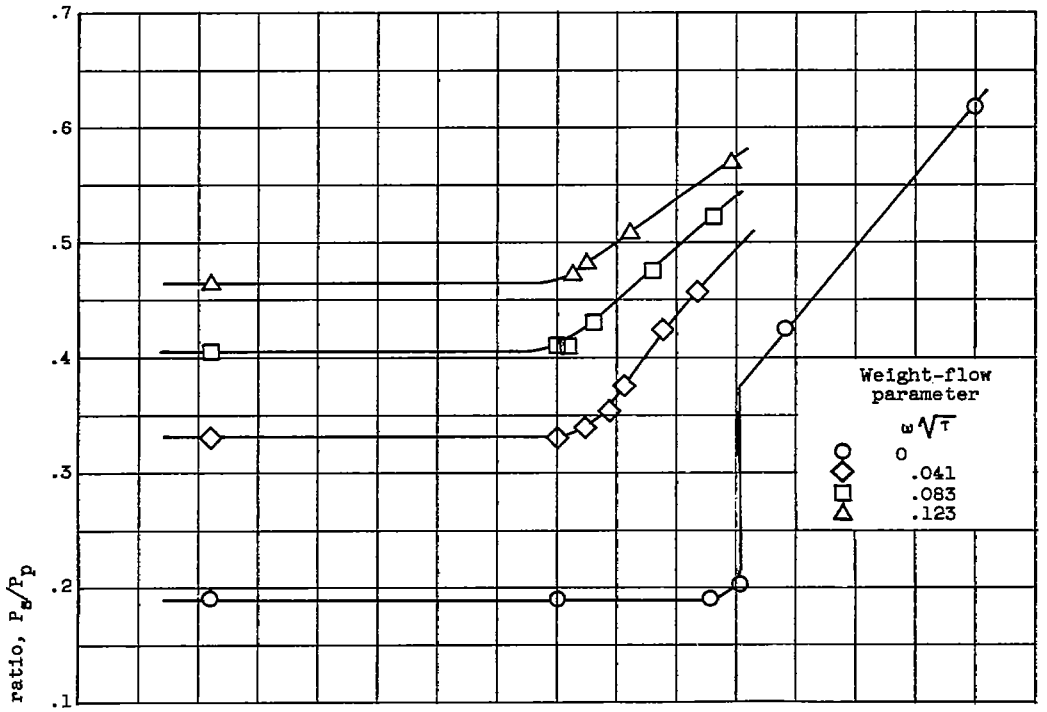

(e) Shroud-length ratio, L/D_p, 1.29.

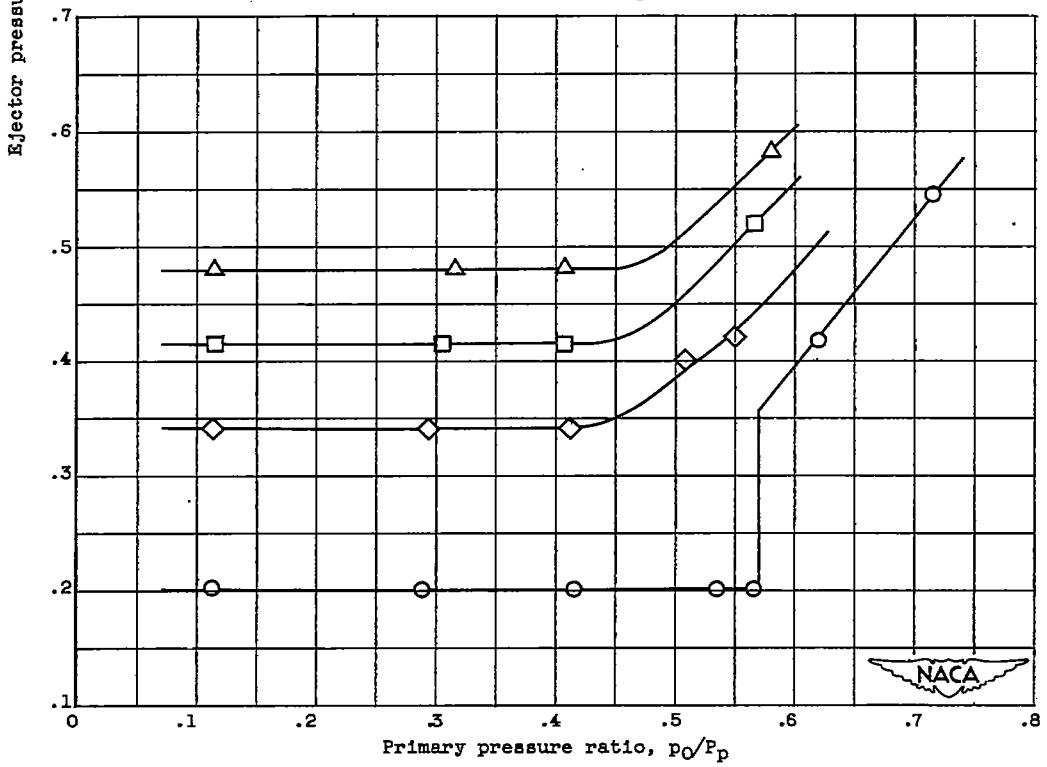

(f) Shroud-length ratio, L/D_p, 1.72.

Figure 4. - Concluded. Ejector performance curves. Diameter ratio D_s/D_p, 1.20.

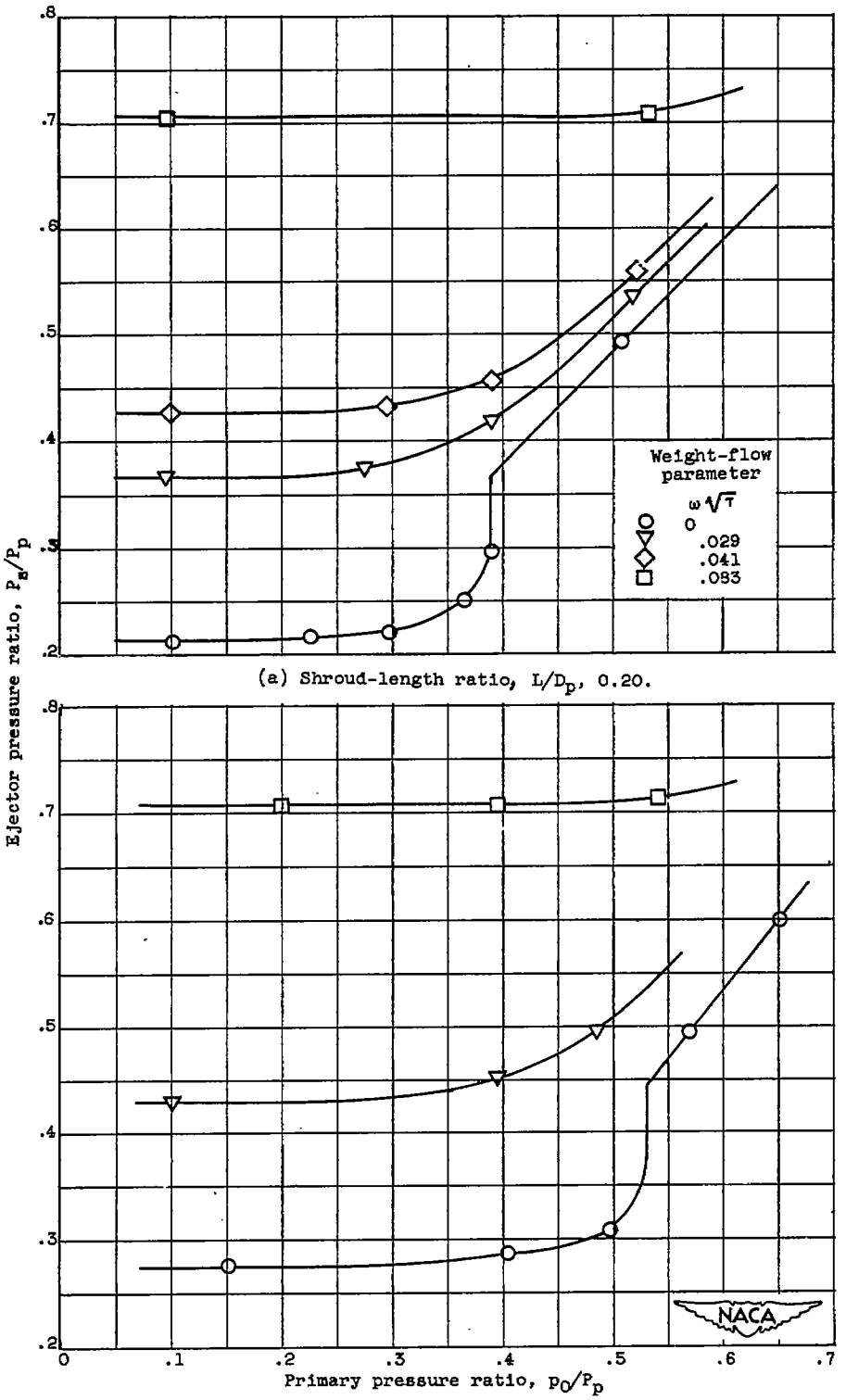

(a) Shroud-length ratio, L/D_p, 0.20.

(b) Shroud-length ratio, L/D_p, 0.39.

Figure 5. - Ejector performance curves. Diameter ratio D_s/D_p, 1.10.

[redacted]

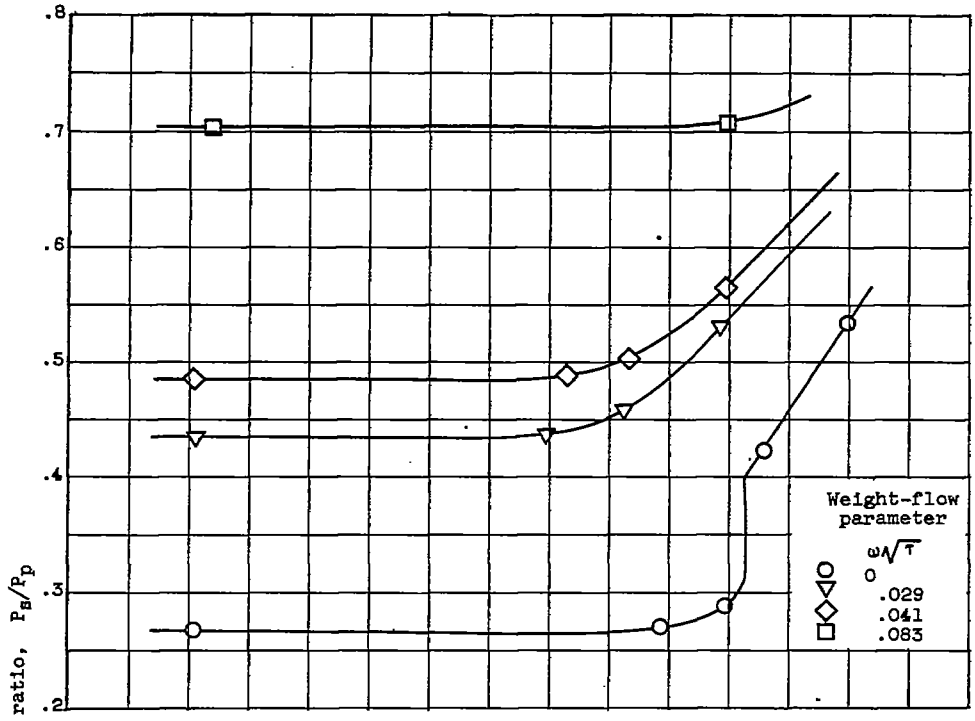

(c) Shroud-length ratio, L/D_p, 0.59.

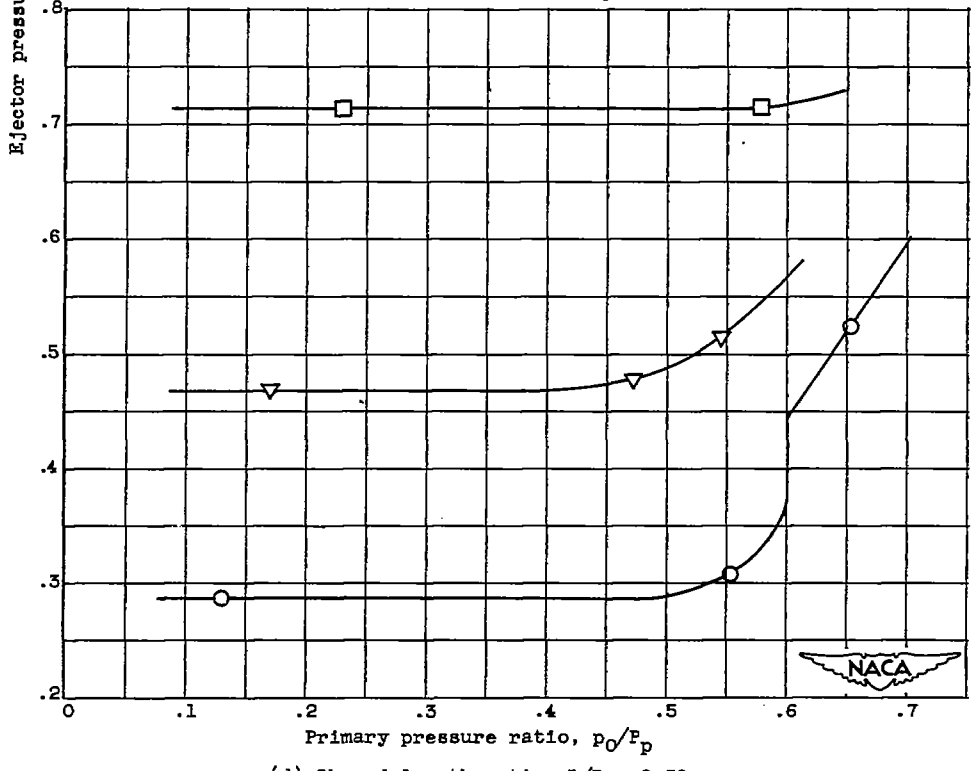

(d) Shroud-length ratio, L/D_p, 0.79.

Figure 5. - Continued. Ejector performance curves. Diameter ratio D_s/D_p, 1.10.

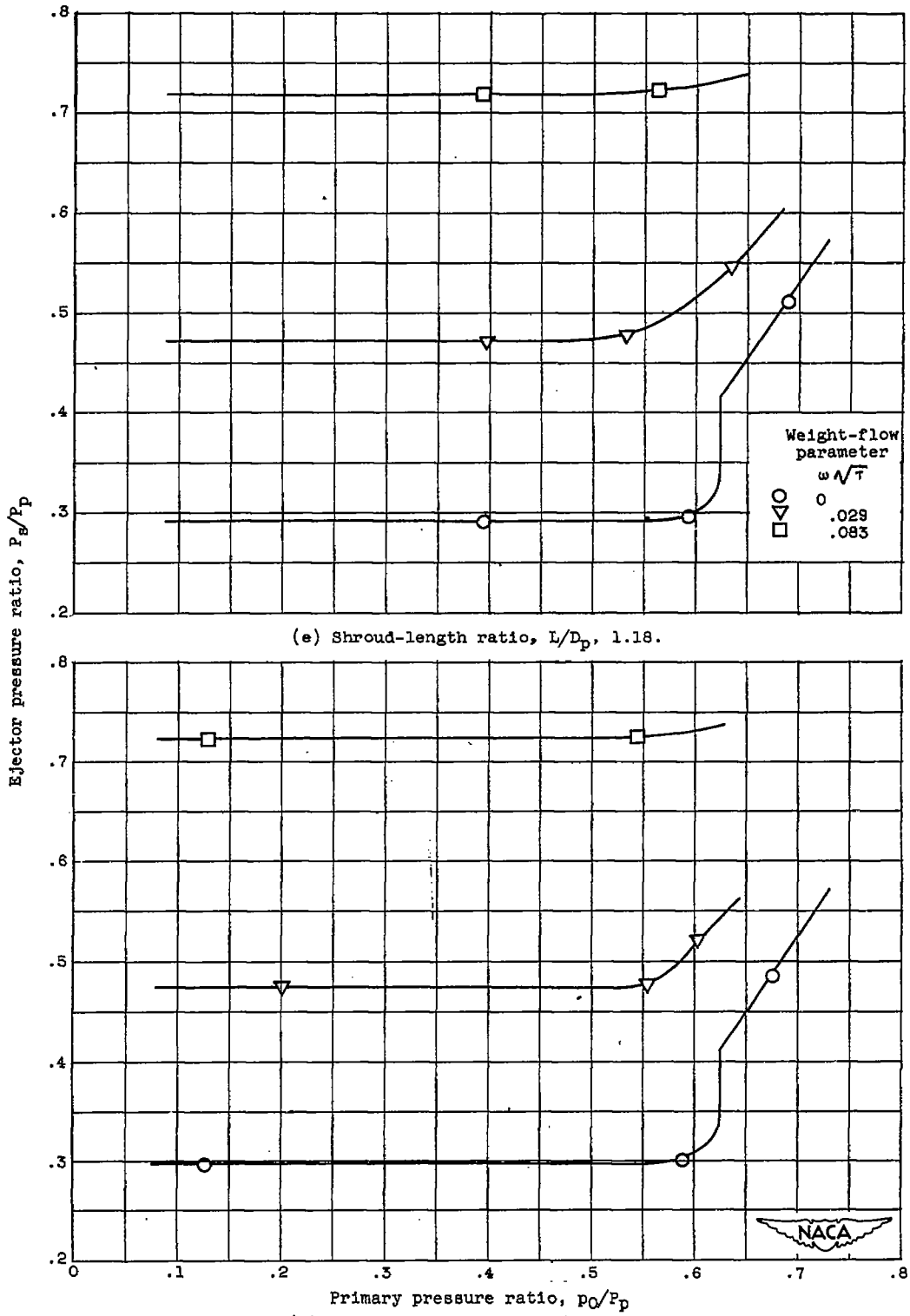

(e) Shroud-length ratio, L/D_p, 1.18.

(f) Shroud-length ratio, L/D_p, 1.57.

Figure 5. - Concluded. Ejector performance curves. Diameter ratio D_s/D_p, 1.10.

[redacted]

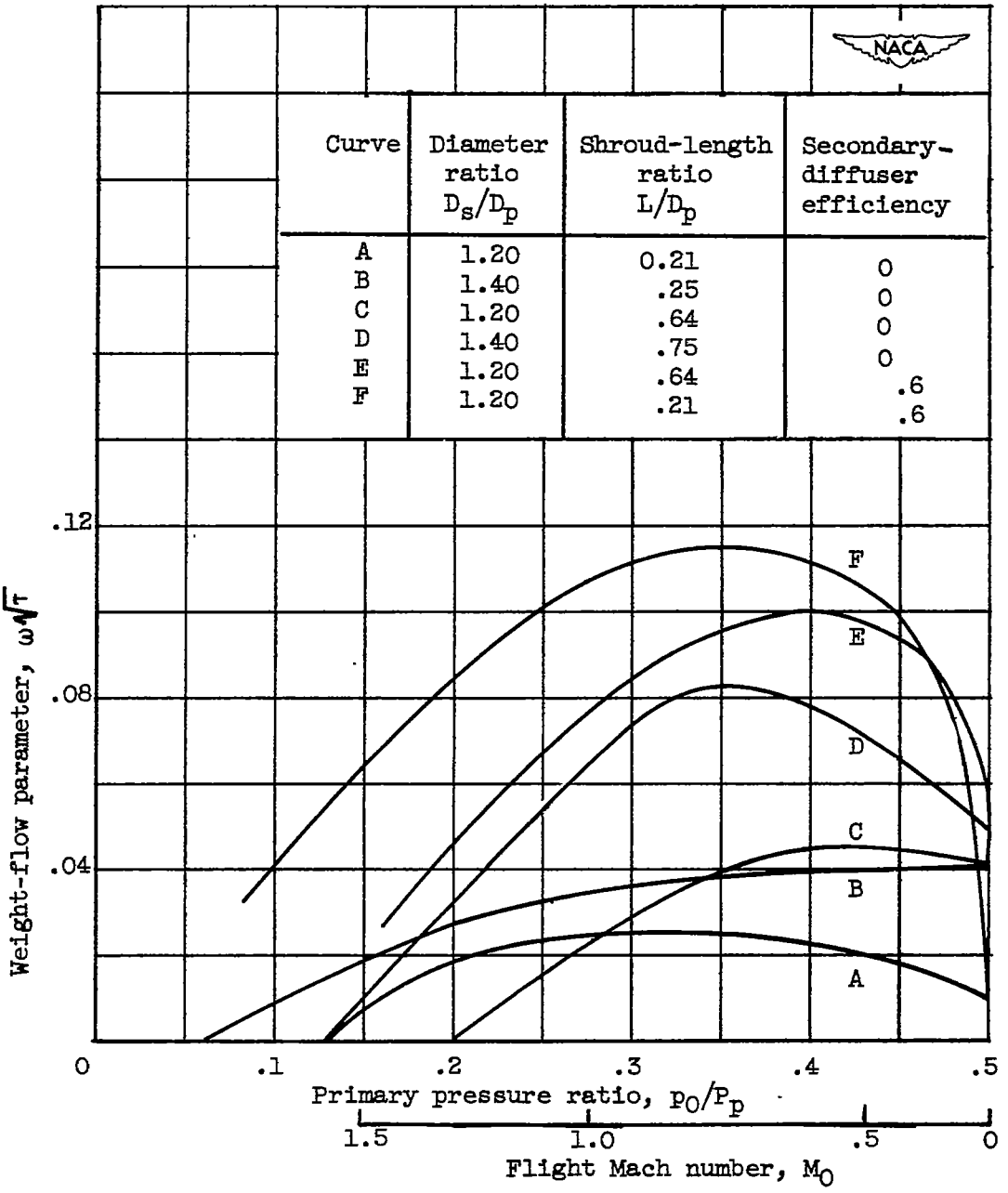

Figure 6. - Variation of weight-flow parameter with primary pressure ratio or flight Mach number for several ejectors. Primary diffuser efficiency, 0.95; engine pressure ratio, 2.0.

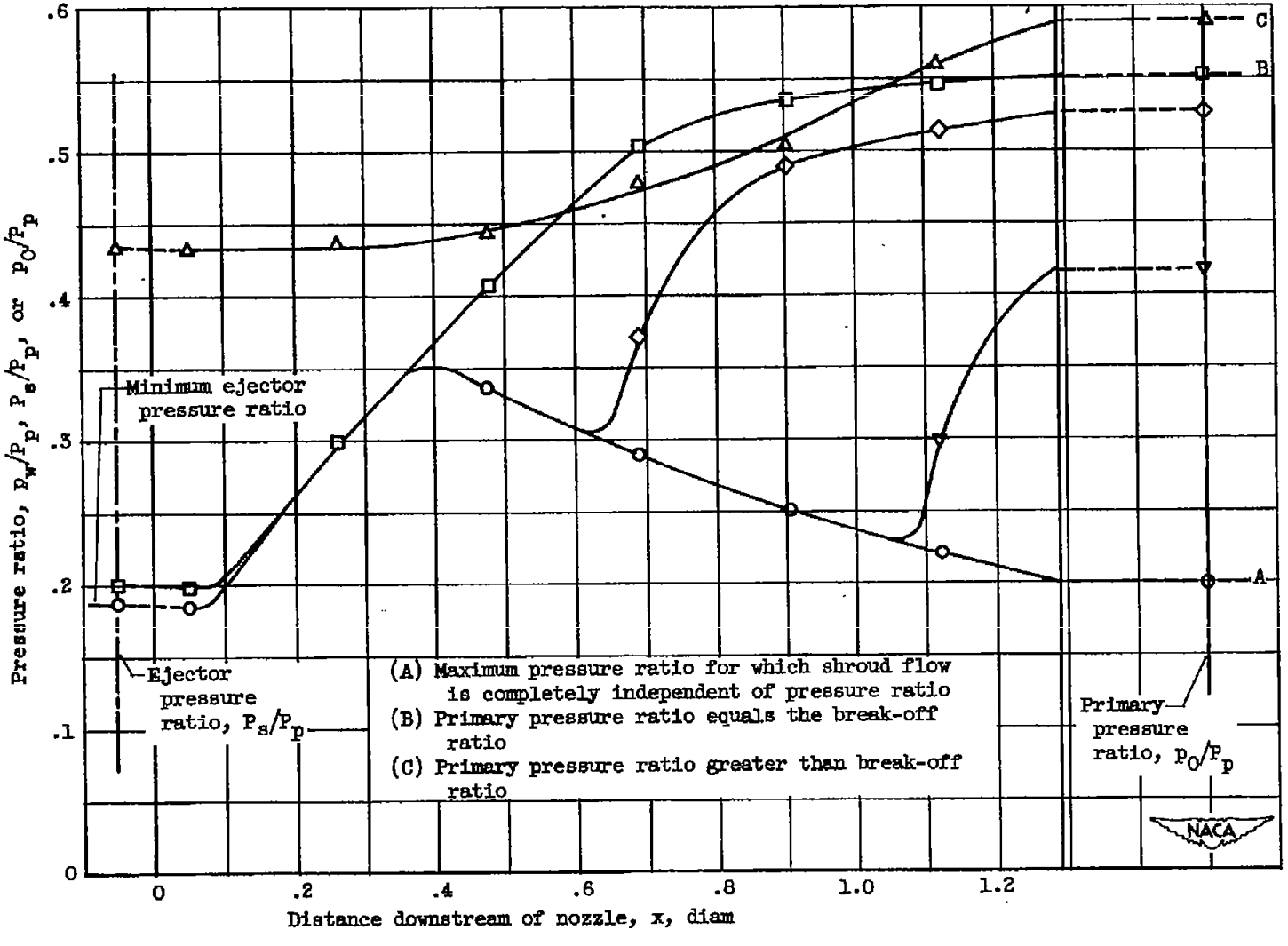

Figure 7. - Typical variation of shroud wall pressure distribution with primary pressure ratio. Diameter ratio D_s/D_p, 1.20; shroud-length ratio L/D_p, 1.29. No secondary flow.

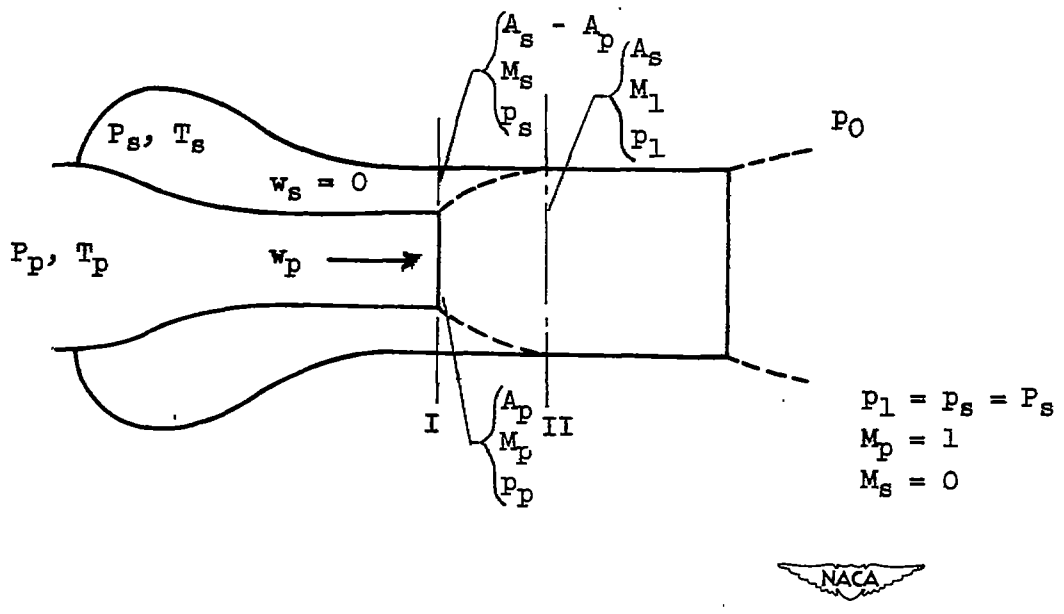

Figure 8. - Schematic diagram of internal flow. No secondary flow.

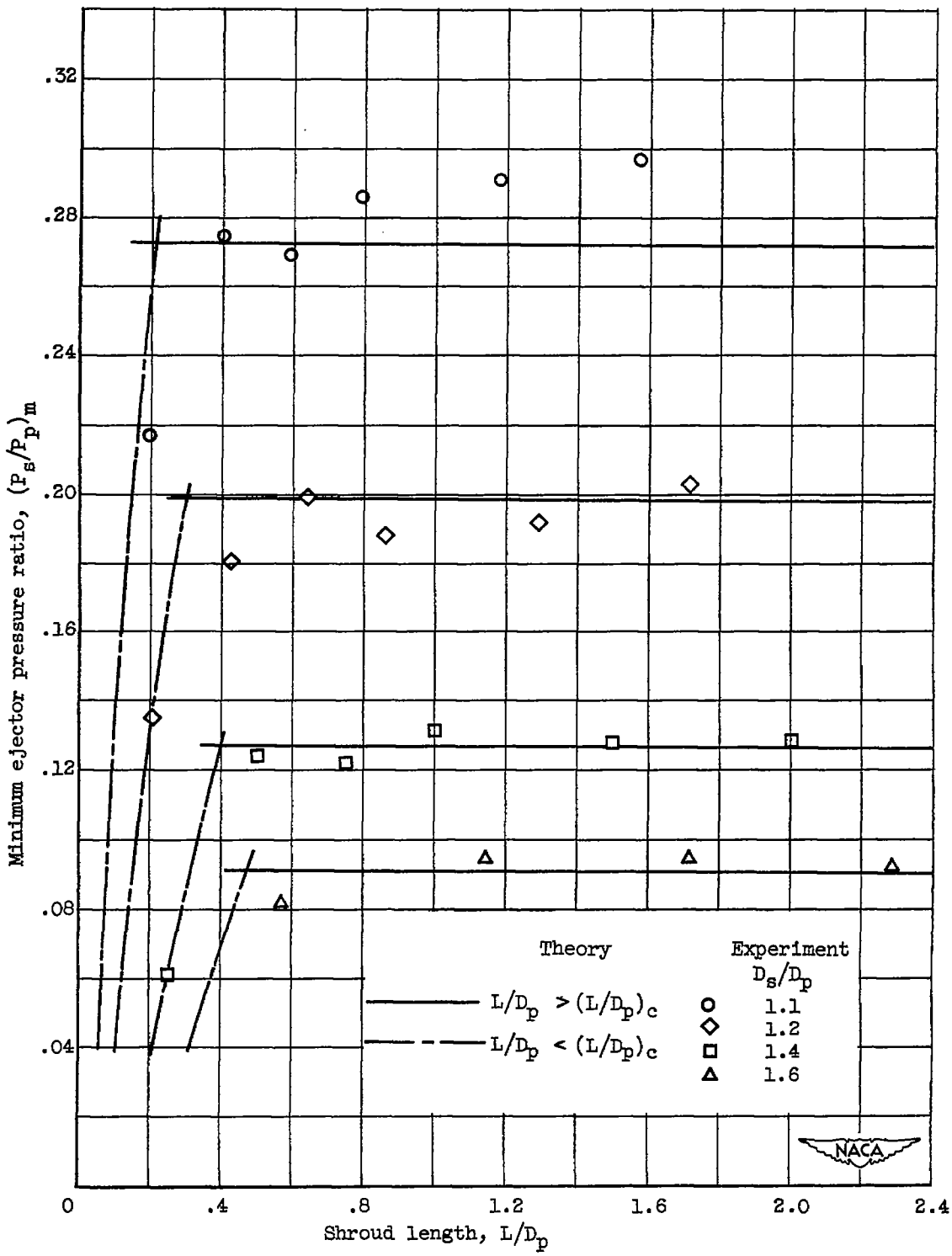

Figure 9. - Theoretical and experimental variation of minimum ejector pressure ratio with shroud length for several diameter ratios. No secondary flow.

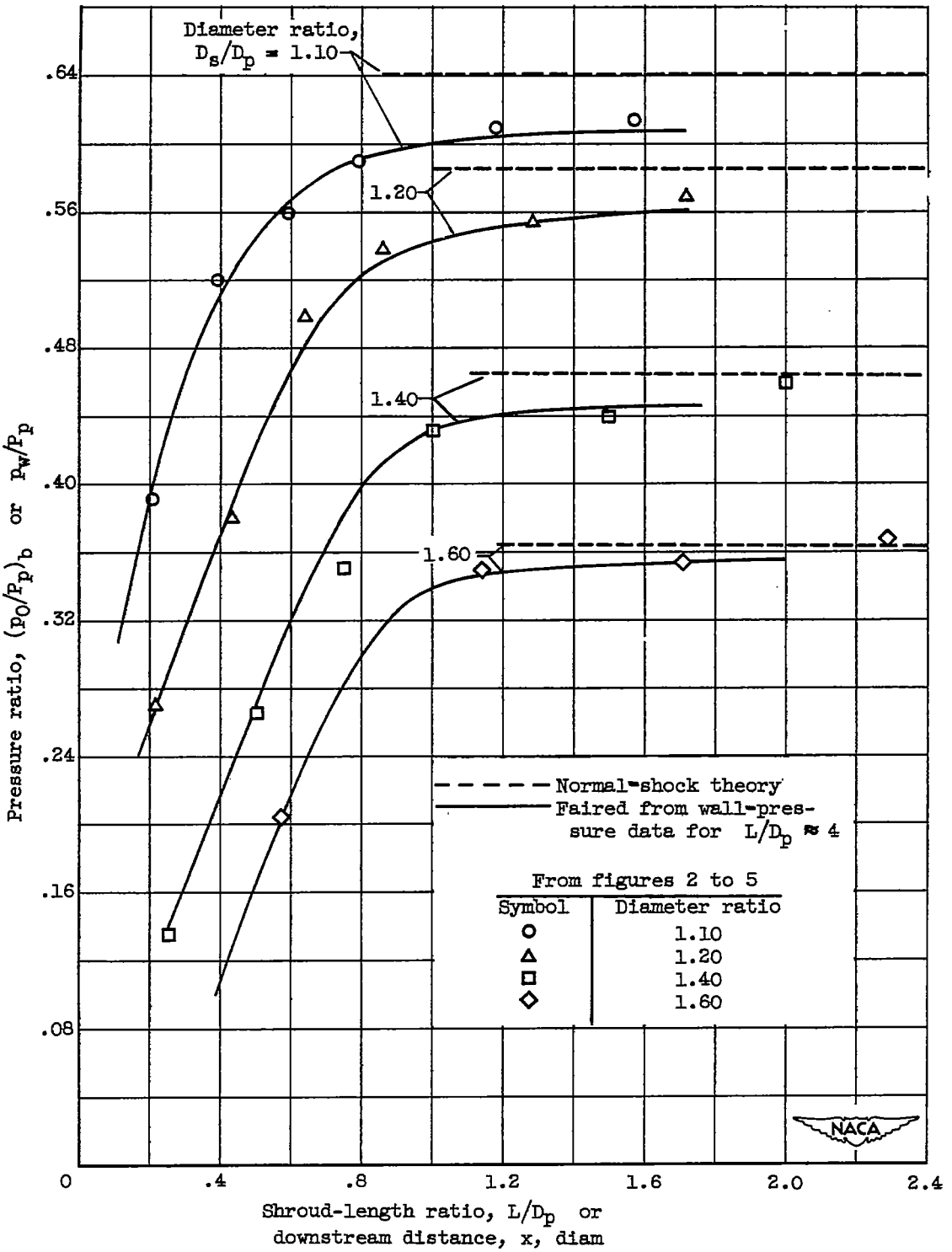

Figure 10. - Theoretical and experimental variation of break-off pressure ratio with shroud length ratio for several diameter ratios. No secondary flow.

[redacted]

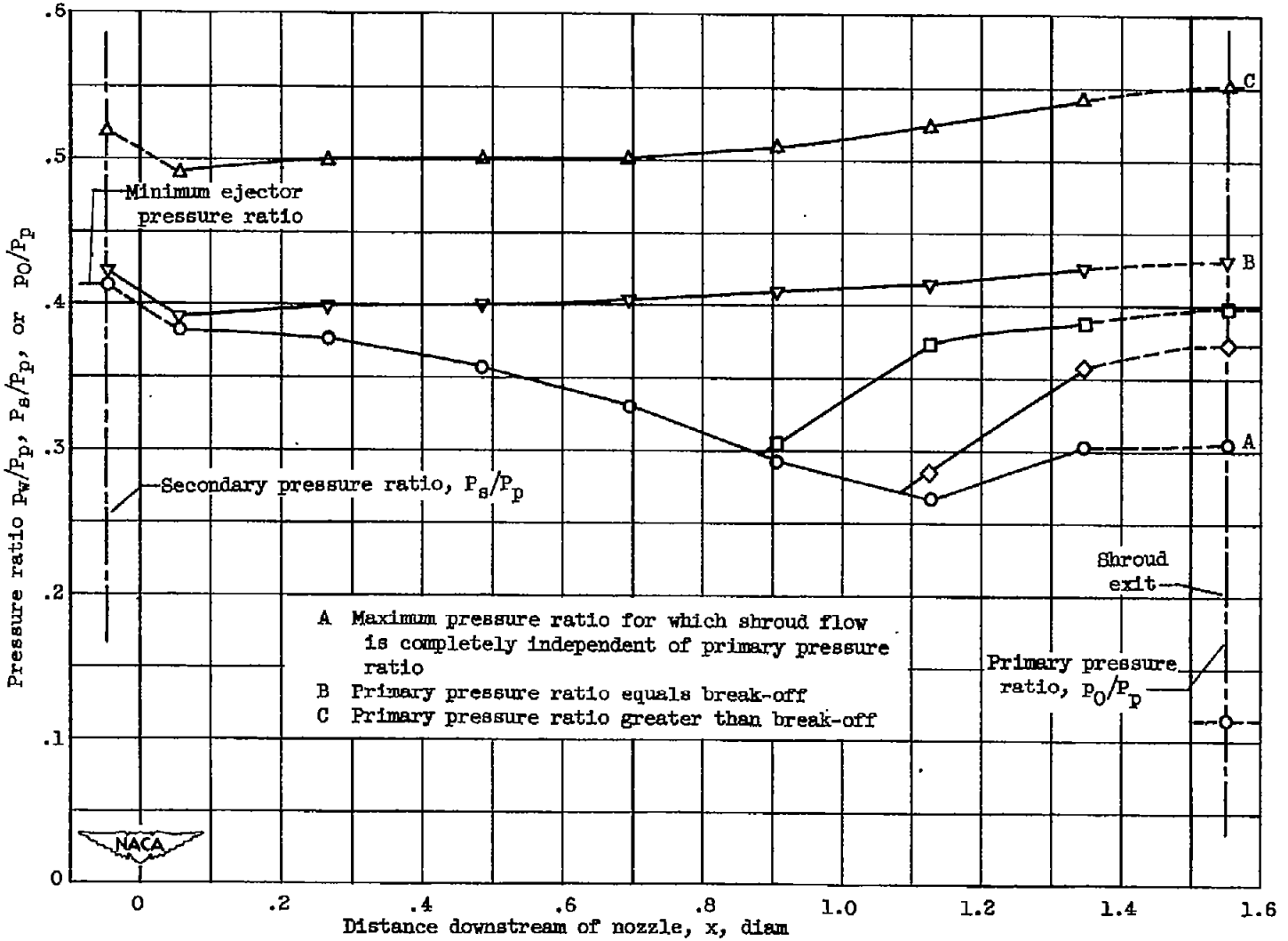

Figure 11. - Typical variation of shroud wall pressure distribution with primary pressure ratio. Weight-flow parameter $\omega\sqrt{T}$, 0.083; diameter ratio D_s/D_p, 1.20; shroud-length ratio L/D_p, 1.29.

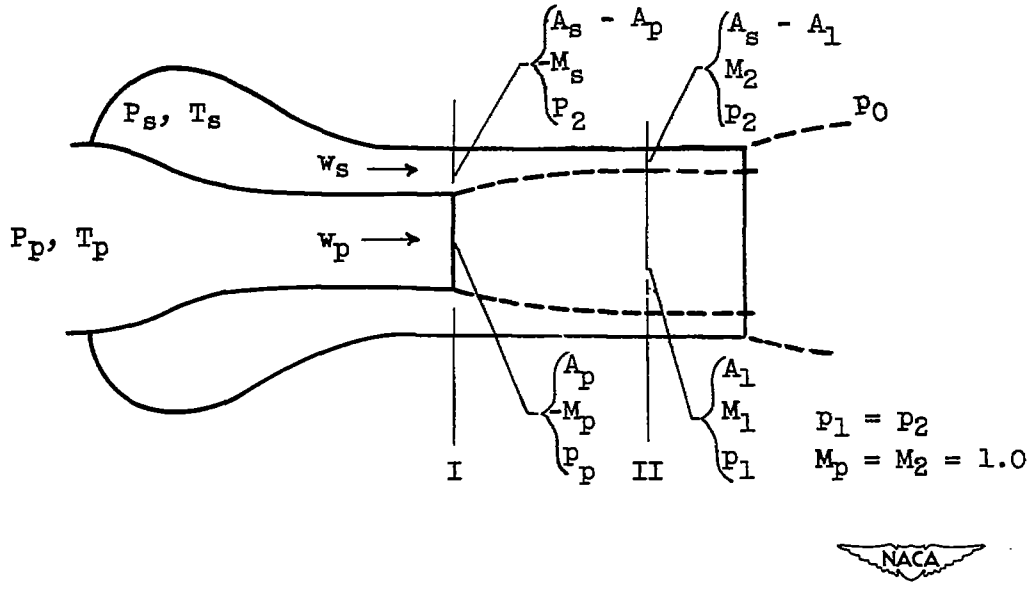

Figure 12. - Schematic diagram of internal ejector flow for case of secondary flow.

[redacted]

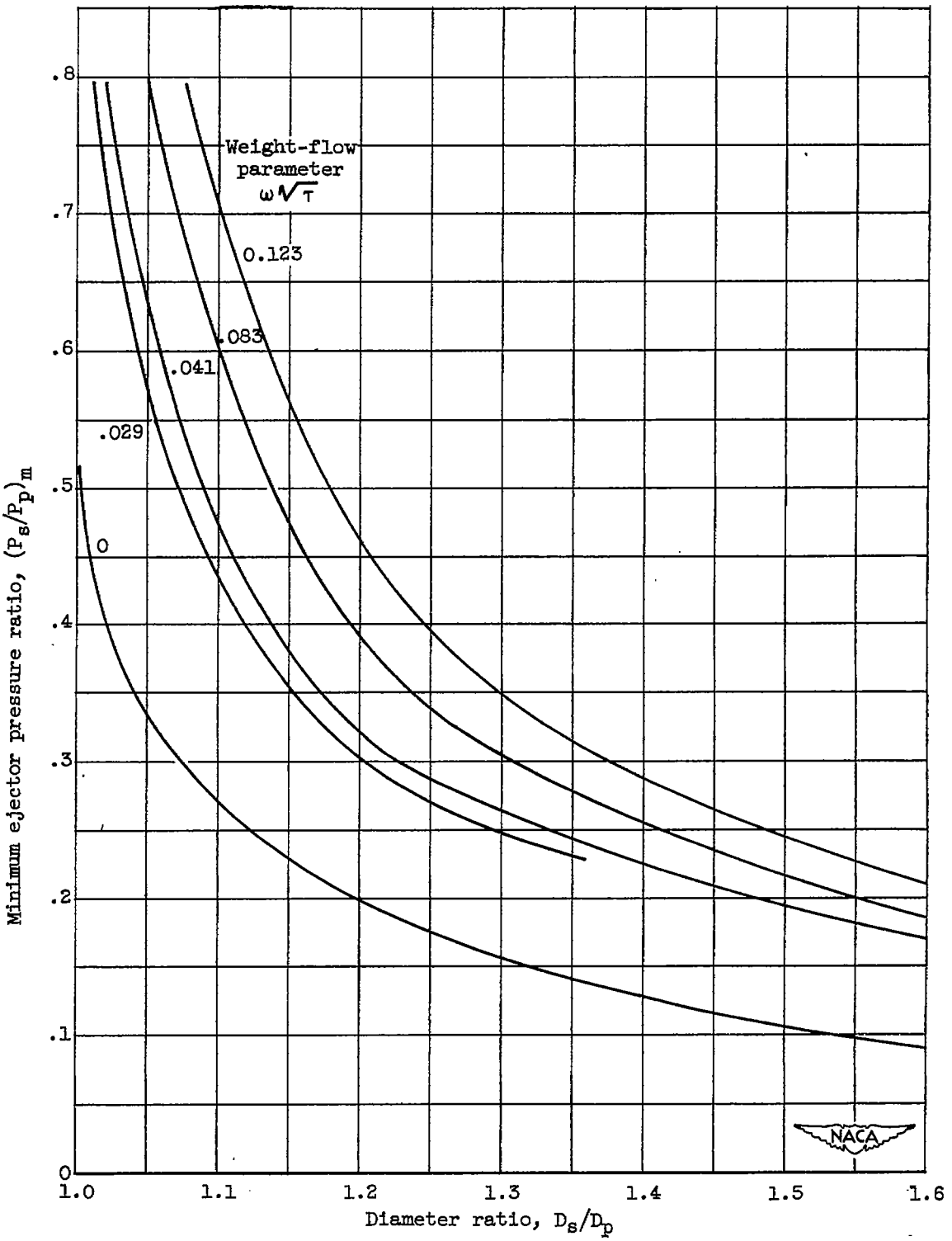

Figure 13. - Theoretical variation of minimum ejector pressure ratio with diameter ratio for several values of weight-flow parameter.

[redacted]

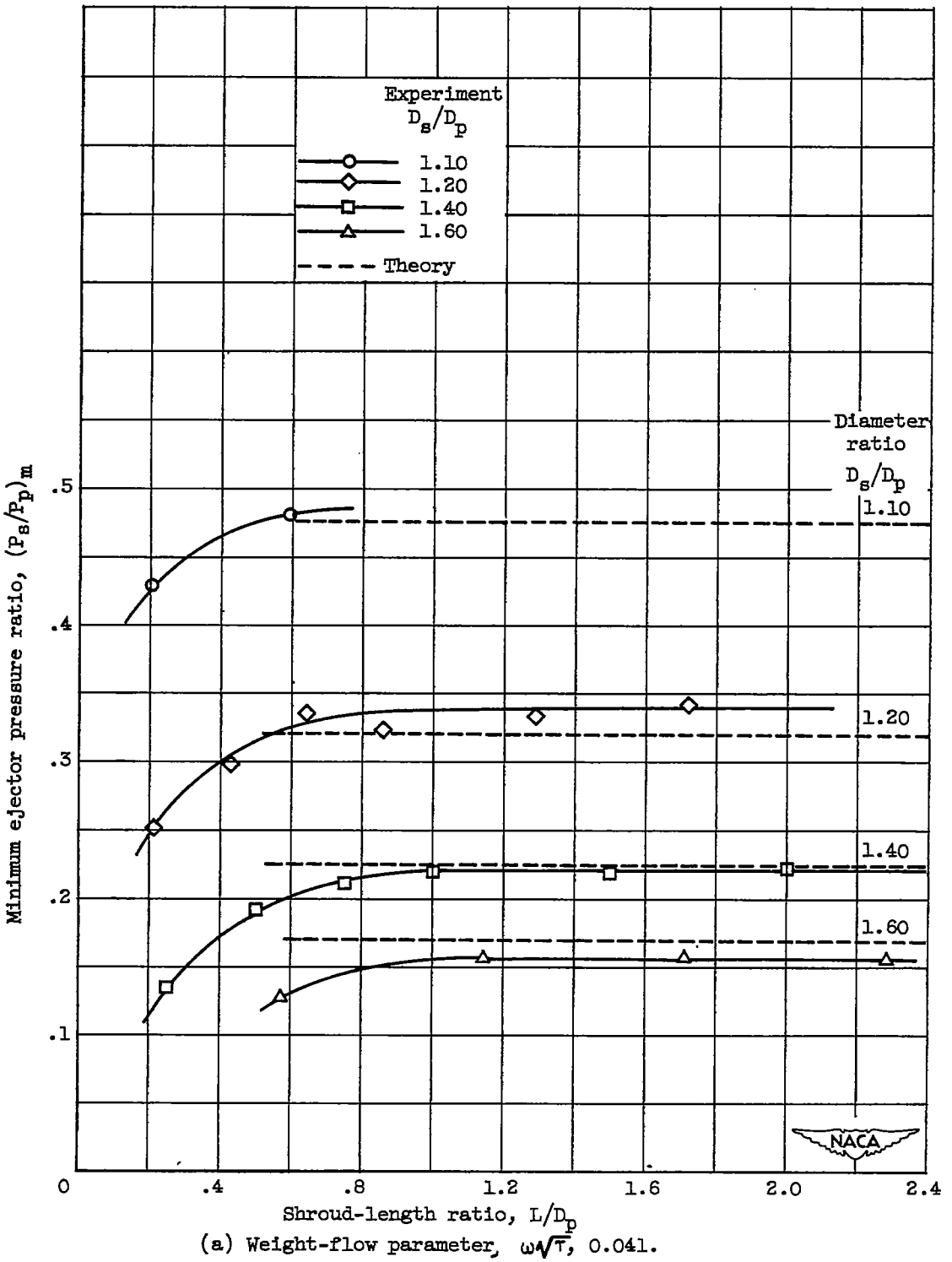

(a) Weight-flow parameter, $\omega\sqrt{\tau}$, 0.041.

Figure 14. - Comparison of theoretical and experimental values of minimum ejector pressure ratio.

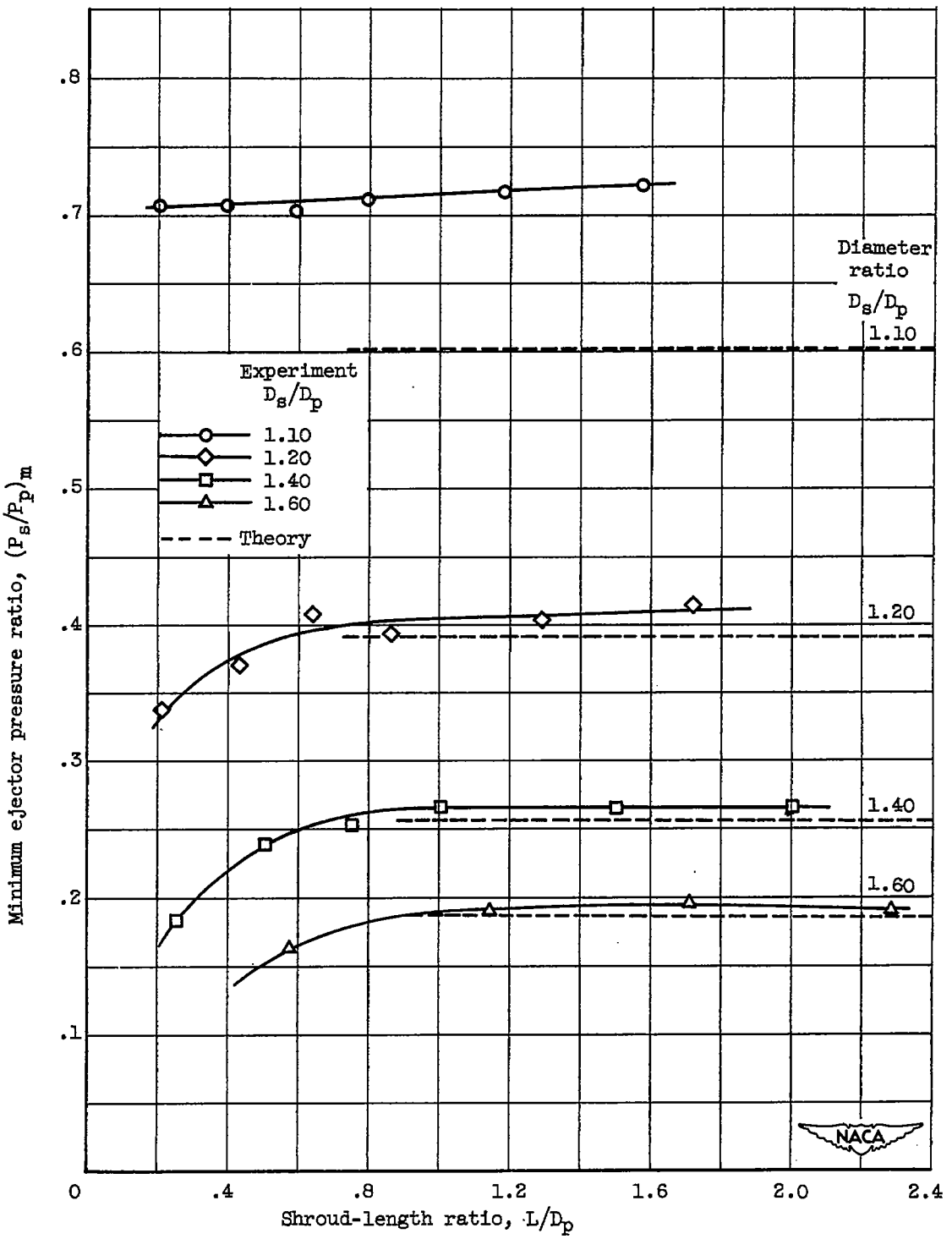

(b) Weight-flow parameter, $\omega\sqrt{\tau}$, 0.083.

Figure 14. - Continued. Comparison of theoretical and experimental values of minimum ejector pressure ratio.

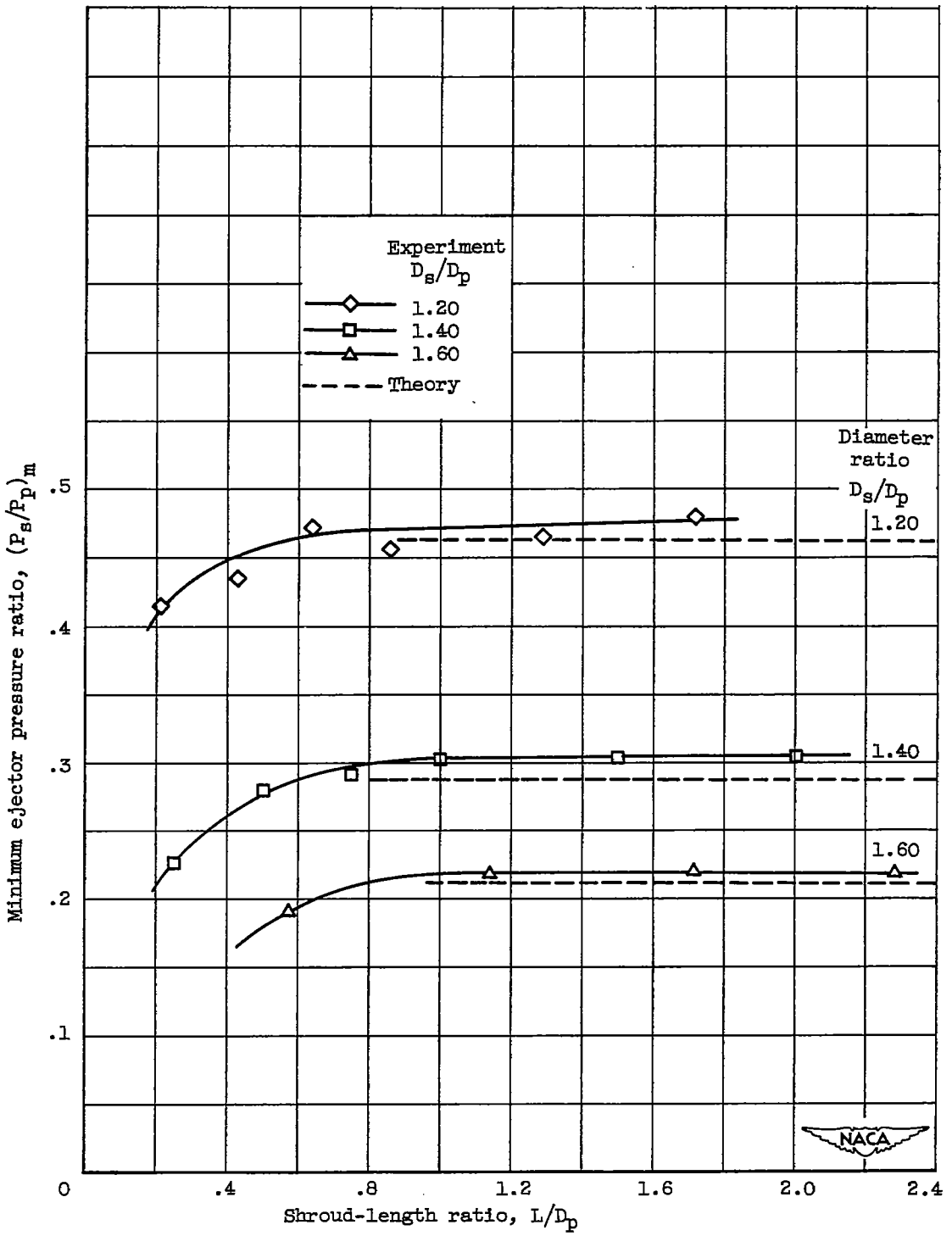

(c) Weight-flow parameter, $\omega\sqrt{\tau}$, 0.123.

Figure 14. - Concluded. Comparison of theoretical and experimental values of minimum ejector pressure ratio.

[redacted]

NACA-Langley - 5-22-51 - 435